2017-05-09 POSTER COPERTINA phd expo 2017.qxp_Layout 1 11/05/17 12:10 Pagina 1

PhD Expo 2017

25 maggio – 5 giugno 2017
Campus Rizzi
via delle Scienze 206
Udine

L'evento, organizzato dall'Università di Udine in collaborazione con l'Acceleratore digitale 'Friuli Innovazione', presenta la vetrina delle attività di ricerca condotte dai dottorandi iscritti al terzo anno dei corsi di dottorato.

Gli obiettivi:
- **comunicare** i risultati di ricerche e progetti
- **condividere** le idee e le proposte
- **confrontare** le esperienze e le competenze
- **contaminare** i diversi saperi

HR EXCELLENCE IN RESEARCH

UNIVERSITÀ DEGLI STUDI DI UDINE
hic sunt futura

FRIULI innovazione®
Centro di Ricerca e di Trasferimento Tecnologico

FONDAZIONE FRIULI

2017-05-09 POSTER NOMI phd expo 2017.qxp_Layout 1 12/05/17 09:20 Pagina 1

PhD Expo 2017

25 maggio – 5 giugno 2017
Campus Rizzi
via delle Scienze 206

Tutti i poster e tutti gli autori
30° ciclo corsi di dottorato

HR EXCELLENCE IN RESEARCH

SCIENZE SOCIALI E UMANISTICHE
SOCIAL SCIENCES AND HUMANITIES

CORSO DOTTORATO SCIENZE GIURIDICHE

BUSET GIACOMO
La concessione in godimento a scopo traslativo

CIMAROSTI ALIDA
Ripensare al *part time*, ripensare il *part time*? Il lavoro a tempo parziale tra sfide demografiche e crisi economica

DELLA TORRE JACOPO
La giustizia negoziata in Europa

MAGGIO IDA CARLA
La connessione impropria e la tutela dei diritti individuali omogenei

MARINO DENISE
I confini del diritto

URBAN FEDERICA
Il potere discrezionale del giudice penale nella definizione della pena e gli automatismi sanzionatori

CORSO DOTTORATO SCIENZE MANAGERIALI E ATTUARIALI

BELFANTI NICOLE
Lean Management come cambiamento organizzativo: le persone contano

CARZEDDA MATTEO
Agrifood systems and sustainability: The role of Alternative Food Networks

DAN NELU
Sentence-based Topic Models Aspect Discovery and Latent Aspect Regression Rating

SLONIMSKAYA ANASTASIYA
Public-private partnership (PPP) in CIS countries – (hard) work in progress

CORSO DOTTORATO STUDI LINGUISTICI E LETTERARI

GESIOT JACOPO
Lelio Manfredi traduttore: la ricezione delle letterature iberiche nell'Italia del primo '500

GIRO ALESSANDRA
I personaggi migranti e la narrazione in prima persona nella letteratura italiana 2001-2014

SIANO PAOLA
Il carteggio Michele Barbi - Ernesto Giacomo Parodi (1895-1922). Personalità, studi e problemi verso la «Nuova Filologia»

CORSO DOTTORATO STUDI STORICO ARTISTICI E AUDIOVISIVI

BONANOMI MATTEO MIRKO
La decorazione pubblica in Italia tra Unità e Prima guerra mondiale

DOTTO SIMONE
***Un moderno sentire*. Culture dei media sonori nell'Italia tra le due guerre.**

PASCALE GUIDOTTI MAGNANI CATERINA
I Guidotti tra arte e società a Bologna (XVI-XVIII secolo)

PERIN CHIARA
Realismo in Italia, 1944-1954

SIARDI MASSIMO
Nuove prospettive per il Digital Heritage italiano tra il 2010 e il 2015

SCIENZE DELLA VITA
LIFE SCIENCES

CORSO DOTTORATO SCIENZE E BIOTECNOLOGIE AGRARIE

CAPPELLETTI MARTINA
Development and assessment of *plant protein hydrolysates as biopesticides* against zucchini powdery mildew

COLUSSI ALICE
Salivary cortisol: a marker of the adaptive response of the dog to different environmental stimuli

DE MORI GLORIA
Fine physical mapping of a resistance region to Sharka (Plum Pox Virus) in apricot

NARDIN TIZIANA
Study of alpine herb alkaloid profiles and research of milk traceability markers by high resolution mass spectrometry

NIKULINA ANNA
Rumen utilization of urea-based feeds by in vitro studies

POLANO CESARE
Next-Generation-Sequencing Metagenomic Analysis of Phytopathogenic Prokaryotes

RUOCCO SILVIA
Improvement of chemical quality index of wines from interspecific hybrids

TACOLI FEDERICO
Grapevine pest management through natural compounds and agronomic practices

Lotta contro i fitofagi della vite con sostanze di origine naturale e pratiche agronomiche

ZULIANI ANNA
Il benessere della bovina da latte: un'opportunità per produttori e consumatori

CORSO DOTTORATO SCIENZE BIOMEDICHE E BIOTECNOLOGICHE

BIASUTTI LEA
Oxidative metabolism during wheelchair propulsion tests in patients with spinal cord injury: effects of lesion level

CANTARUTTI CRISTINA
Citrate-stabilized gold nanoparticles hinder fibrillogenesis of a pathological variant of β2-microglobulin

CUTANO VALENTINA
Investigating the role of HDAC7 in the control of mammary gland morphogenesis and transformation

DE ZUANI MARCO
Mast cells during *Candida albicans* infections: new insights for an old player in fungal clearance

DONGMO FOUMTHUIM CEDRIX JURGAL
Molecular dynamics simulations of β2-microglobulin interaction with hydrophobic surfaces

MALFATTI MATILDE CLARISSA
Repair of modified ribonucleotides embedded in DNA

MIGLIETTA GIULIA
Development of anti-cancer therapies targeting RAS oncogene through non-canonical RNA structures.

TECNICO SCIENTIFICA
PHYSICAL SCIENCES AND ENGINEERING

CORSO DOTTORATO INFORMATICA E SCIENZE MATEMATICHE E FISICHE

ANTICOLI LINDA
Entangλe: from Quantum Programming to Quantum Model Checking

BASALDELLA MARCO
Extracting (key|technical) terms from scientific documents

LIESSI DAVIDE
Pseudospectral methods for the stability of linear periodic delay models

PERESANO MICHELE
Very high zenith angle observations of the Crab Nebula with MAGIC telescopes

SILVETTI SIMONE
Verification and Validation of Complex Systems

CORSO DOTTORATO INGEGNERIA INDUSTRIALE E DELL'INFORMAZIONE

ARRIGONI FEDERICA
Synchronization of Multiple Views

BADAMI OVES
Numerical Modeling of Multigate nano-FETs

BANDIZIOL ANDREA
Design of an interface for high-speed serial links in automotive micro-controller

CITOSSI MARCO
Biomass Characterization for Solar Pyrolysis

GANIS ALEXANDER RUDOLF
Architectures and Algorithms for the Signal Processing of Advanced MIMO RADAR Systems

KAPIDANI BERNARD
Explicit Time-Domain Full Maxwell Solvers over Tetrahedral Grids

KRAS ALEKSANDER
Flywheel Inertial Transducer For Energy Harvesting And Vibration Control

PESSOT ELENA
La Valutazione della Complessità nei Progetti e l'Influenza sull'Apprendimento

TURCO EMANUELE
Noise and vibration control of cylindrical structures with tuneable vibration absorbers

VACI LUBOS
Context-Based Goal-Driven Reasoning for Improved Target Tracking

YAKUSHEVA NADEZDA
An ADAS Design Based on IoT V2X Communications

ZIENTEK MICHAL WLADISLAW
Metamaterial panel with piezoelectric patches connected to multi-resonat electrical shunts

CORSO DOTTORATO SCIENZE DELL'INGEGNERIA ENERGETICA E AMBIENTALE

AHMADI SOMAYEH
Wall transform mechanism in a viscosity stratified turbulent flow

GAGLIARDI ANDREA
Structured Approach to the Failure Analysis

MASSOLINO GIULIA
Methodological proposal for the preliminary dynamic assessment of soil-structure interaction on energy production and distribution facilities through ambient vibration tests

PAGNACCO FABIO
Analisi delle prestazioni termiche in sistemi di raffreddamento avanzati di palette di turbine a gas

ROCCON ALESSIO
Coalescence & breakage of drops in turbulence

SUZZI NICOLA
Numerical Simulation of Thin Film Breakup on Non-wettable surfaces

TOSO ALESSANDRA
Pd/CeO2 based catalysts: resistant materials for methane emissions abatement from NGVs

VECLANI DANIELE
Nano Strutture per Macro Problemi: Nano-Tubi di Carbonio per la Rimozione di Antibiotici

UNIVERSITÀ DEGLI STUDI DI UDINE
hic sunt futura

FRIULI innovazione®
Centro di Ricerca e di Trasferimento Tecnologico

FONDAZIONE FRIULI

Development and assessment of *plant protein hydrolysates as biopesticides* against zucchini powdery mildew

M. Cappelletti, M. Perazzolli, A. Nesler, O. Giovannini, I. Pertot

INTRODUCTION

The substitution of synthetic chemical pesticides has become a priority in agriculture, and the induction of plant resistance by protein hydrolysates may offer a sustainable solution. Based on literature data, the efficacy of protein hydrolysates is affected by the origin, the method and the degree of hydrolysis, as well as by the amino acid and peptide composition.

The aim of this work was to clarify the effect of enzymatic and acid hydrolysis on different plant protein sources (soybean, rapeseed and guar protein meals), in term of efficacy against the powdery mildew of zucchini (caused by *Podosphaera xanthii*).

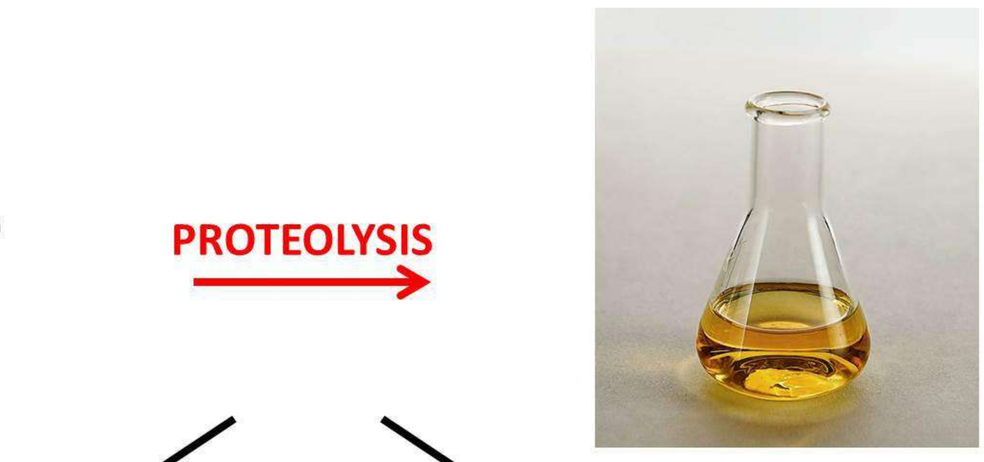

ENZYMATIC hydrolysis (50°C, 24 h)

- Enzymes: Alcalase and Flavourzyme
- E/S ratios: 1% and 50%

CHEMICAL hydrolysis with sulfuric acid H_2SO_4

- Condition A: 121°C, 15 min
- Condition B: 100°C, 8 h

RESULTS and DISCUSSION

Preventive foliar treatments with guar hydrolysates produced with both Alcalase 50% and with H_2SO_4 6N B significantly reduced disease symptoms compared to the non-hydrolysed protein source, and the biocontrol effect was related to the degree of hydrolysis, and peptide and amino acids content.

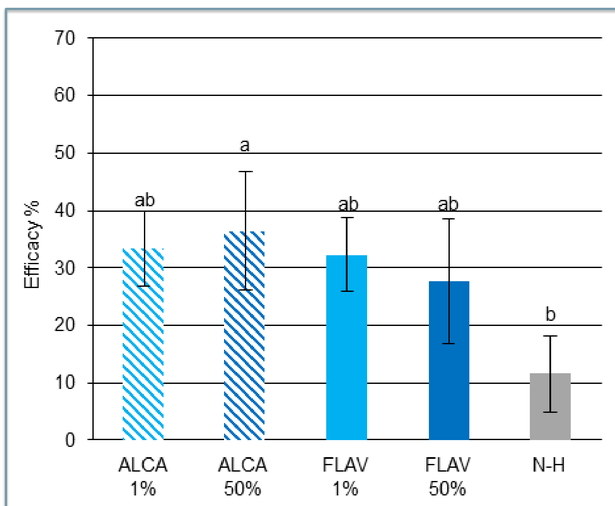

FIGURE 1. Efficacy % of guar enzymatic hydrolysates against powdery mildew was evaluated on zucchini plants treated with hydrolysed and non-hydrolysed (N-H) protein sources as compared to water-treated plants. Enzymatic hydrolysates were obtained using Alcalase (ALCA) and Flavourzyme (FLAV) at dosage of 1% (ALCA 1% and FLAV 1%, respectively) and 50% of the protein content (ALCA 50% and FLAV 50%, respectively). Different letters indicate significant differences among treatments according to Fisher's LDS test ($p \leq 0.05$).

However, the use of strong acids such as H_2SO_4 during the hydrolysis causes an increase of salinity of protein hydrolysates, and the significant efficacy of guar acid hydrolysates against the disease was largely caused by the formation of **potassium sulphate**, which is a common fertilizer.

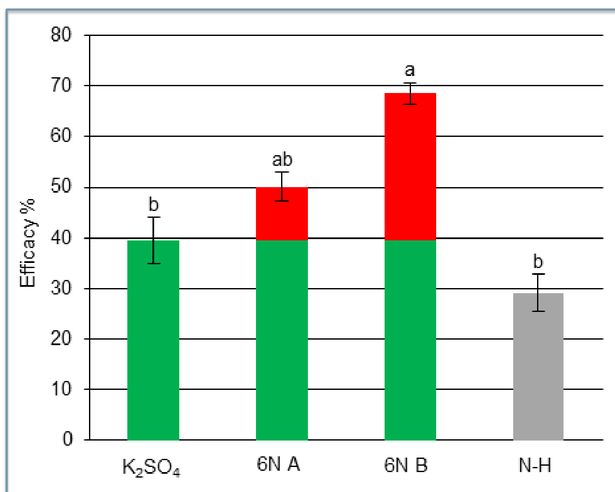

FIGURE 2. Efficacy % of guar acid hydrlolysates against powdery mildew was evaluated on zucchini plants treated with hydrolysed and non-hydrolysed (N-H) protein sources or with 0.11 M K_2SO_4 as compared to water-treated plants.. Acid hydrolysates were obtained by incubation of protein source with 6 N H_2SO_4 at 121°C for 15 min (6N A) and at 100°C for 8 h (6N B). Different letters indicate significant differences among treatments according to Fisher's LDS test ($p \leq 0.05$). For each hydrolysate, the contribution of **K_2SO_4** and **hydrolysed proteins** to the efficacy in disease reduction was visually presented through **green** and **red** bars, respectively.

CONCLUSIONS

Fighting crop diseases through the foliar application of low-cost protein hydrolysates represent an innovative research field, and it may play a role in integrated pest management programs for making agriculture more sustainable, reducing negative drawbacks of traditional chemical. However, further studies are required to clarify their mechanisms of action in relation to their composition, such as gene expression analysis and effects on phyllosphere microbial communities. Moreover, other specific trials are needed to evaluate their stability and efficacy under field conditions.

PhD Candidate: *Dott. Martina Cappelletti*
Supervisor: *Prof. Ilaria Pertot*
Co-supervisor: *Dott. Michele Perazzolli*

Contacts:
tel: +39 0461 615506
mail: cappelletti.martina@spes.uniud.it
ilaria.pertot@fmach.it

References

-Walters DR *et al.* (2013) J Exp Bot 64:1263-1280
-Albert M (2013) J Expl Bot 64:5269-5279
-Colla G *et al.* (2015) Sci Hort 196:28-38
-Nesler A *et al.* (2015) Front Plant Sci 6:715
-Cappelletti M *et al.* (2016) Front Plant Sci 7:1053

Acknowledgements

The project has been funded with support from *Fondazione Edmund Mach* (San Michele all'Adige, Trento)

UNIVERSITÀ DEGLI STUDI DI UDINE
hic sunt futura

LIFE SCIENCES

30° ciclo
Corso di dottorato in Scienze e biotecnologie agrarie

SALIVARY CORTISOL: A MARKER OF THE ADAPTIVE RESPONSE OF THE DOG TO DIFFERENT ENVIRONMENTAL STIMULI

INTRODUCTION

The interest for dog well-being has dramatically increased over the past decades and attracted researchers to develop methods aimed at explaining the interaction between animal genetic and behavioral response with environmental stimuli. Cortisol is the key effector molecule of the hypothalamic-pituitary-adrenal (HPA) axis and its concentration can be measured in different matrixes, but saliva and hair are the most suitable non-invasive matrixes for this purpose In addition, salivary cortisol, with a delay of 20-30 minutes, shows a high correlation to plasma cortisol level *(Vincent et al.,* 1992; *Beerda et al.,* 1998).

STUDY 1 Effect of different factors on the variations of salivary cortisol of healthy dogs

We recruited 92 dogs from private owners (13), kennels (4), and shelters (2). For each dog, 3 samples were collected during the same day (Figure 1). The T0 sample was collected before the morning meal (6:00-8:00 AM), right after the first interaction of the day with the owner and T1 sample 30 minutes after the meal. The last sample (T2) was collected 30 minutes after the last interaction of the day with man, when dogs were resting and relaxed.

Figure 1**.** Sampling saliva in a dog.

To collect the saliva the swab should be kept in the dog's mouth for 15-20 seconds two- three times.

RESULTS

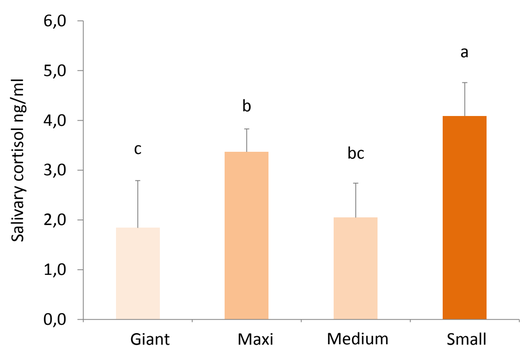

Figure 2. Differences in salivary cortisol levels (ng/ml) in relation to size.

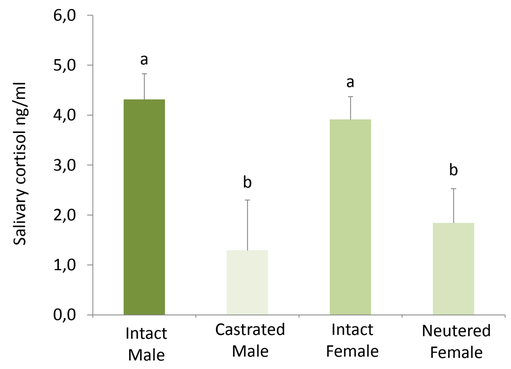

Figure 3. Differences in salivary cortisol levels (ng/ml) in relation to sexual status.

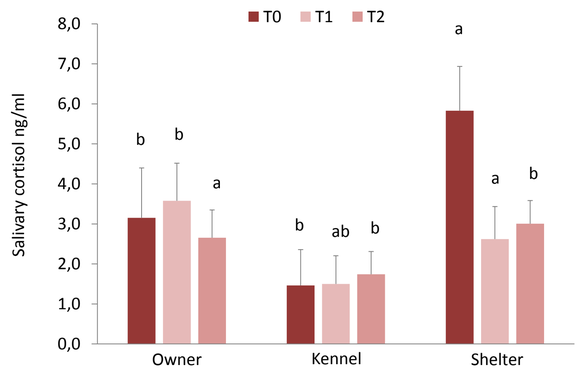

Figure 4. Differences in salivary cortisol levels (ng/ml) in relation to environment and time of day.

In this study we observed that cortisol concentrations significantly differed between small-sized dogs and other sizes (Figure 2), castrated/spayed animals and intact dogs (Figure 3) and the time of sampling in different environments (Figure 4).

In conclusion, size of dogs, sex, and time of sampling in different environments have to be considered as factors that can influence basal cortisol values in the saliva (*Colussi et al.,* 2016; *Sandri et al.,* 2015).

STUDY 2 Salivary cortisol as biomarker to monitor physiological response to different conditions

We assessed the variation of salivary cortisol in dogs that were trained for 5 activities: Pointing Hunting, Tracking for Ungulate Hunting, Blood Tracking, Agilty Training and Animal Assisted Activity (AAA). For each dog, 3 samples were collected. A baseline sample (T0) was collected from all the dogs, at the evening before the day of activity, 30 minutes after the last interaction of the day with man, when dogs were resting and relaxed. For all the dogs recruited, a second salivary sample (T1) was collected just before the beginning of activity and a third salivary sample (T2) was collected roughly at 15 minutes from the end of the session**.**

RESULTS

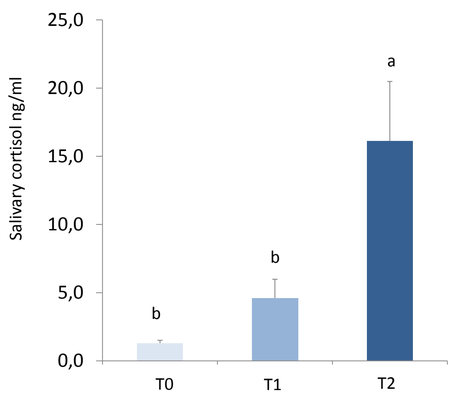

Figure 5. Variation of salivary concentrations of cortisol (ng/ml) measured in dogs during Pointing Hunting session.

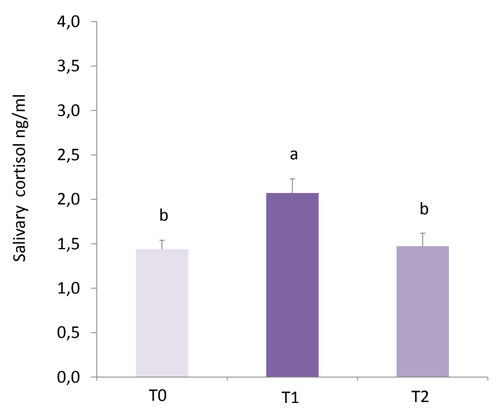

Figure 6. Variation of salivary concentrations of cortisol (ng/ml) measured in dogs during Animal Assisted Activity (AAA) session.

In this preliminary study we observed that cortisol concentration significantly differed between times of sampling in Pointing Hunting (Figure 5) and in AAA session (Figure 6).

In conclusion, salivary concentration of cortisol response to different activities varied in relation to the type, the extent and the level of alertness that was requested from the performance.

FUTURE PERSPECTIVES

- Application of salivary cortisol as a mean to evaluate canine HPA axis activation, to predict the ability of the animal to cope with environmental stimuli.
- Investigation of the relationship between cortisol concentration and other factors, as breed predisposition to different activities.

PhD Student: **Alice Colussi**
Supervisor: **Prof. Bruno Stefanon**
Info: +39 0432 558573
colussi.alice.1@spes.uniud.it

BIBLIOGRAPHY

Beerda B, Schilder MB, van Hooff JARAM, de Vries HW, Mol JA. Behavioural, saliva cortisol and heart rate responses to different types of stimuli in dogs. Applied Animal Behaviour Science 58:365-381, 1998.

Colussi A, Sandri M, Stefanon B. Salivary cortisol: a marker of the adaptive response of the organism to environmental stimuli. Veterinaria Vol 30, Issue 3, 2016.

Sandri M, Colussi A, Perrotta MG, Stefanon B. Salivary cortisol concentration in healthy dogs is affected by size, sex, and housing context. Journal of Veterinary Behavior: Clinical Applications and Research 10:302-306, 2015.

Vincent IC, Michell AR. Comparison of cortisol concentrations in saliva and plasma of dogs. Research in Veterinary Science 53(3):342- 345, 1992.

UNIVERSITÀ DEGLI STUDI DI UDINE
hic sunt futura

LIFE SCIENCES
30° ciclo
Corso di dottorato in Scienze e biotecnologie agrarie

Fine physical mapping of a resistance region to Sharka (Plum Pox Virus) in apricot

Gloria De Mori[1], Rachele Falchi[1], Rachele Messina[1], Raffaele Testolin[1], Simone Scalabrin[2], Marco Passaro[3], Filippo Geuna[3], Daniele Bassi[3], Federica Savazzini[4], Luca Dondini[4], Stefano Tartarini[4]

INTRODUCTION

Plum Pox Virus (PPV) is the causative agent of Sharka, a severe disease of stone fruit (apricot, plum, almond, peach and cherry). Unlike other plant pathogens, PPV cannot be directly controlled by chemicals and the isolation of genes for resistance would represent a good control of this disease with significant economic and environmental benefit. The resistance to PPV has been studied extensively in apricot and a main QTL associated to resistance has been mapped on the upper part of the chromosome one (LG1) (Dondini *et al.*, 2011).

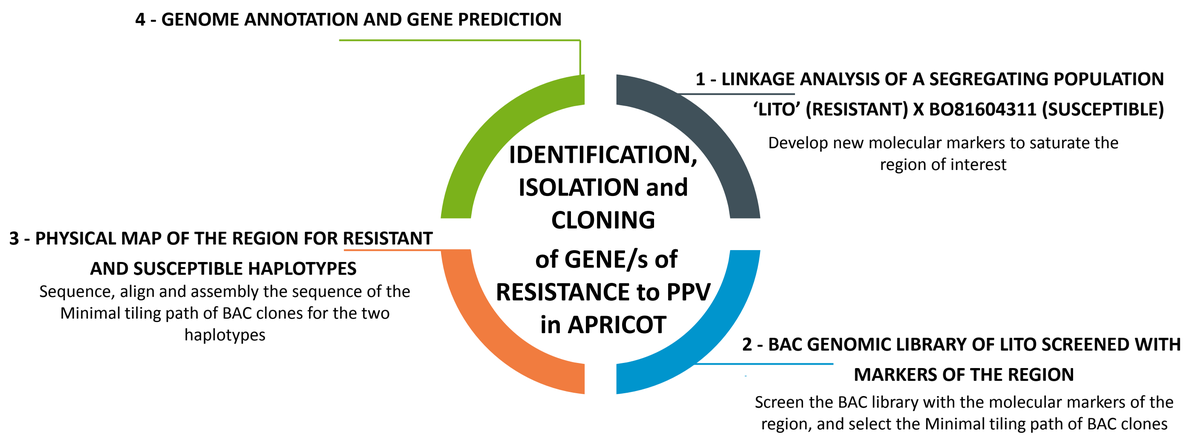

RESULTS

- 47 new markers (19 SCAR/SSR from the peach genome scanned with Sputnik software and 28 SNPs developed from the Lito BAC sequences) were mapped either on R and S chromosome by Sequenome analysis. The new set of markers identified was used to saturate the genetic map and to perform a three-dimensional pooling of the 'Lito' BAC library.
- 26 positive BAC clones were selected that covered the resistant haplotype and 30 for the susceptible one. BACs were sequenced with NGS platform, aligned with Dot Plot and assembled with iAssembler software using clones overlap, regardless of the peach genome. This process allowed the reconstruction of the largest part of the two haplotypic regions (resistant and susceptible), with a few gaps.
- The assembly of the BAC sequences was hampered by the presence of several repeated regions and many BAC sequences are still fragmented in various contigs which order cannot be disambiguated.
- The peach genome served initially as a good-guideline but the contigs order was not solved in apricot regions lacking collinearity with the peach genome

FUTURE PROSPECTS

- The reconstruction of Both R and S haplotypic sequences of chromosome 1 carrying the gene of resistance of Sharka is being completed by sequencing the whole Lito genome using PacBio technology.
- Genome annotation and prediction of candidate gene/s for resistance to PPV in apricot has been initiated.
- Marked assisted selection (MAS) in breeding programs is being developed using the new markers tightly linked to the candidate R gene.

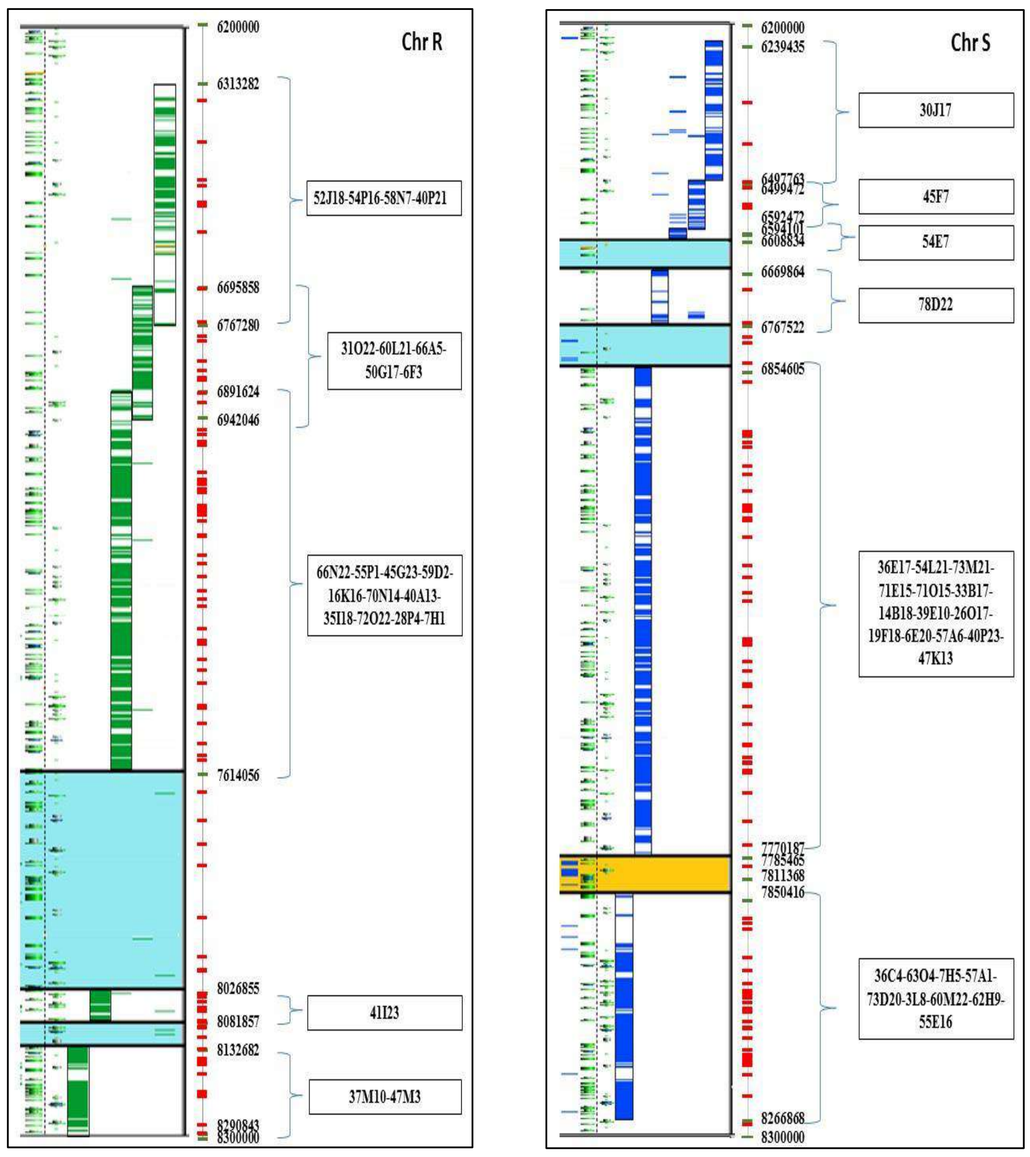

SUPERCONTIG	LENGTH
52J18-54P16-57N7-40P21	256767
31O22-60L21-66A5-50G17-6F3	227866
66N22-55P1-45G25-28D2-16K16-70N17-40A13-35I18-72O22-28P4-7H1	692568
41I23	66958
37M10-47M3	151245
ChrR total length	1398404

SUPERCONTIG	LENGTH
30J17	155480
45F7	84371
54E7	82267
78D22	90949
36E17-54L21-73M21-71E15-71O15-33B17-14B18-39E10-26O17-19F18-6E20-57A6-40P23-47K13	834395
36C4-63O4-7H5-57A1-73D20-3L8-60M22-62H9-55E16	381462
ChrS total length	1628924

Figure 1: The region of interest (6.2 to 8.3 Mbp) of the LG1 showing the position of Lito BAC supercontigs aligned to the peach sequence (green the resistant haplotype and blue the susceptible one). On the left the output of Gevo_sequence software (https://genomevolution.org/CoGe/GEvo.pl) is shown. Markers that saturate the region of interest are reported in red, following their physical distance in peach genome. The regions lacking of coverage are highlighted in light blue color. Yellow area in susceptible haplotype evidences a possible inversion found in apricot chromosome with respect to peach.

Dott.ssa Gloria De Mori
Prof. Raffaele Testolin
Info:
Tel. +39 0432 558646
Indirizzo mail
demori.gloria@spes.uniud.it

Acknowledgments

[1]University of Udine, Udine, Italy
[2] IGA Technology Services, Udine, Italy
[3] University of Milan, Milan, Italy
[4] University of Bologna, Bologna, Italy
CNR Virology Institute, Bari

UNIVERSITÀ DEGLI STUDI DI UDINE
hic sunt futura

LIFE SCIENCES

30° ciclo

Corso di dottorato in Scienze e biotecnologie agrarie

Study of alpine herb alkaloid profiles and research of milk traceability markers by high resolution mass spectrometry

Tiziana Nardin[ab], Edi Piasentier[b], Roberto Larcher[a]

a Centro Trasferimento Tecnologico, Fondazione E. Mach, via E. Mach 1, 38010 San Michele all'Adige (TN), Italia.
b Dipartimento di scienze agrarie ed ambientali (DISA), Università di Udine, Via Sondrio 2A, 33100 Udine (UD), Italia.

Introduction

In the last few decades over ten thousand alkaloids, an extremely varied group of natural, nitrogen-containing, basic organic compounds, have been isolated from natural sources, mainly in Angiosperms [1]. Alkaloiks are supposed to be waste products of plants metabolic processes and derive from amino acids or from amination of another type of substrate (acetate, phenylalanine, terpene or steroid). A screening method that automatically combinine online solid-phase purification of samples with high resolution mass spectrometry was developed and used for investigate the targeted and untargeted alkaloid profiles of a selection of 80 alpine single herbs, 48 herbal mixes fed by 8 cows, and 48 milk samples collected from the same animals. The migration of alkaloids in milk was evaluated to asses the use of alkaloids as possible milk origin traceability markers.

Materials and methods

80 individual herbal plants of the typical alpine flora, were sampled in Friuli Venezia Giulia (North-West Italy). In same pastures samples of herbage consumed by 8 previously selected cows were collected (48 samples) and, twice a day for 3 days, individual milk were milked from the same cows (48 samples). For herb samples, 2.5 g were added to 20 mL of extraction solution (H2O/MeOH/FA; 44.5:44.5:1 v/v/v) in polyethylene 50 mL tubes, sonicated for 10 minutes, and left under vertical shaking for 12 hours at 20 rpm. The mixtures were once again sonicated for 10 minutes, and the methanolic extract was separated after centrifugation (10 minutes at 4100 rpm), filtered with a 0.45 µm cellulose filter cartridge and diluted twice with water. For milk samples, 5 g were added to 2 mL of extraction solution (H2O/MeOH/FA; 40:40:20 v/v/v) in polyethylene 50 mL tubes and sonicated for 15 minutes. Then 1 mL hexane was added and the samples were shaken for 10 minutes. After centrifugation (10 minutes at 4100 rpm) the hexane phase was removed and the water layer was filtered with a 0,45 µm cellulose filter cartridge and diluted twice with water.

On-line concentration/purification was performed with a SolEx HRP SPE cartridge, while the chromatographic separation was carried out on a Raptor Biphenyl analytical column in 25 minutes [5]. The mass spectrometer was operated in positive ion mode and mass spectra were acquired in full MS-data dependent MS/MS analysis at mass resolution of 140.000.

Forty-one alkaloids were quantified with reference to pure analytical standards. Further 116 (Table 1) were putatively identified on the basis of accurate mass, isotopic pattern, chromatographic retention time and fragmentation profile, obtained by analysing the extracts of herbs already well documented in the literature [3].

Results

The method was linear up to alkaloid concentrations of 400/1000 µg L^{-1} with R2 always > 0,99, and detection limits ranged from 0.1 to 5 µg L^{-1} (Table 1). As regards single herbs content, Figure 1 shows the profiling of alkaloids sorted by chemycal/botanical groups. Piperidines (27 alkaloids), isoquinolines (20), pyrrolizidines (18) and quinolines (16) were the most abundant groups. Differences among the most representative plant flamilies for alkaloid profiles were evaluated according to Tuckey's HSD test ($p<0.05$). E.g. Voacarpine, Caryachine, Parfumidine, Plantagonin, Indicain and 3-Acethyltropine reported significant differences between Plantaginaceeae and all the other families. Concerning pasture and milk samples, Figure 2 reports the alkaloid profiles of the two pastures and the milk collected from cows which grazed on those meadows. For some alkaloids there was a cows which grazed on those meadows migration from herbs to milk (e.g. Stachidrine and Valerianine), furthermore Chinchonanine was present only in one of the two pasture and the corresponding milk samples, while Galegin/Peganin and Magnoflorine were found in the other pasture and milk samples.

Table 1a

Plant	Alkaloid	RT (min)	fragment (m/z) 1	fragment (m/z) 2
Ruta graveolens	Rutacridone	25.4	278.0825	290.1169
	Arborinine	25.4	271.0864	253.0729
	Evoxanthine	13.34	108.0446	158.0598
Eschzhia californias	Sanguinarine	25.3	304.0961	317.0373
	N-Methyllaurotetanine	17.5	280.1089	296.1037
	Caryachine	14.5	281.0865	252.0703
	Caryachine	16.48	295.0993	188.0704
	Caryachine	17.8	311.1334	244.15536
	Caryachine	19.34	295.0885	190.0876
	Escholtzina	18.54	293.0863	188.0704
	o-Methylcaryachine	15.99	295.0957	263.07
	o-Methylcaryachine	18.26	309.1112	188.0702
	Protopin	17.45	148.0595	189.0782
Passiflora incarnata	Harmalol	11.3	144.9972	187.0076
	Harmaline	11.8	197.1071	70.0655
	Norharmane	14.2	81.0722	109.0647
	Harmol	14.4	130.1111	199.0862
	Harmine	15.0	213.1017	195.0867
	Harmane	15.5	91.0857	173.0803
	Harmane	15.9	95.0857	123.0805
Salvia officinalis	Heimidine	21.2	408.2260	/
	Heimidine	22.3	408.2258	/
Glycyrrhiza glabra	Mexacorine	16.3	70.0656	130.0862
	Mexacorine	16.6	70.0658	130.0865
	Acorine	17.3	84.0817	141.1016
	Acorine	17.5	84.0820	141.1016
Ginkgo biloba	Ginkgotoxin	5.46	152.0719	134.0596

Plant	Alkaloid	RT (min)	fragment (m/z) 1	fragment (m/z) 2
Fumaria officinalis	Fumaropyrine	10.6	338.1377	277.0851
	Chelanthifoline	17.2	178.0833	151.0724
	Fumaricine	18.3	309.0755	352.1535
	Fumaritine	18.3	336.1228	323.0901
	Fumaroline	18.3	337.1299	322.1435
	Parfumidine	18.9	58.0657	323.0909
	Sinactine	19.1	324.1221	309.0942
	Sitiopyne	19.2	336.8412	232.9228
	methyl-Fumaropyrine	19.3	277.0855	249.0906
	Parfumidine	19.7	58.0657	323.0909
	Cordalmine	22.4	293.1339	336.1599
Galega officinalis	Galegin /Peganin	15.6	231.62611	259.1478
	Galegin /Peganin	15.9	231.6262	
Vaccinium myrtillus	Myrtine /Epimyrtine	6.9	89.056	151.0961
Piper nigrum	Dihydropiperlonguminine	22.6	155.0436	161.0594
	piperlonguminine	23.0	201.0541	135.0438
	Piperanine	25.1	203.1059	135.0438
	Pipenine	25.5	201.0542	135.0438
Mentha piperita	Lasiocarpine N-oxide	19	254.1374	410.2173
Urtica dioica	Senecophylline N-oxide	22	263.7915	138.0357
Achillea millefolium	Stachydrine	3.5	127.0864	110.0601
	Stachydrine	4.06	127.0865	110.0602
	Betonicine	3	72.0812	132.1014

Table 1b

Plant	Alkaloid	RT (min)	fragment (m/z) 1	fragment (m/z) 2
Geltsemium sempervirens	Gelsemine	11.85	70.0654	236.1065
	Gelsempervine-A / Gelsempervine-C	15.52	180.1016	166.0852
	Gelsempervine-A / Gelsempervine-C	15.62	180.1014	321.1606
	19-epi-voacarpine	16.30	321.1591	206.9741
	19-epi-voacarpine	17.40	321.1591	206.9741
	Gelsempervine-B / Gelsempervine-D	18.54	172.0741	158.06
	Gelsempervine-B / Gelsempervine-D	18.91	172.0737	158.0596
	Gelsemicine	19.59	299.1399	84.0807
	14,15-dihydroxygelsenicine / Gelsenoxonine	28.37	/	/
Hyoscyamus niger	Anisodamine	10.36	140.106	122.0965
Lobelia inflata	8 Ethylnorlobelol	5.60	84.9599	140.1424
	8,10-Diethyllobelidiol	13.05	98.0962	226.2176
	8,10-Diethylobelidiol	13.07	81.0704	220.2148
	8-Methyl, 10-phenyllobelidiol /Norlelobaninine	15.53	196.1076	138.127
	8-Methyl, 10-phenyllobelidiol /Norlelobaninine	16.08	156.1178	171.1374
	Isolobinanidine / Lobinanidine/beta-Lobinanidine	16.23	168.1375	96.0807
	8-Methyl, 10-phenyllobelidiol /Norlelobaninine	16.60	156.1178	171.137
	Lelobaninine I / Lelobaninine II	16.84	162.0893	111.08052
	Isolobinine / Lobinine	16.91	170.154	202.158
	Isolobinanidine / Lobinanidine/beta-Lobinanidine	17.40	90.0655	164.1063
	Isolobinine / Lobinine	17.41	170.1536	202.158
	Isolobinanidine / Lobinanidine/beta-Lobinanidine	17.94	90.0655	168.1375
	Norisolobaninine	19.76	122.0964	105.0699
	Lelobaninine I / Lelobaninine II	19.99	162.0893	111.08052
	cis-Lobelanidine/ trans-Lobelanidine	20.17	202.1584	218.15441
	cis-Lobeline / trans-Lobeline	20.23	216.1361	96.0808
	cis-Lobeline / trans-Lobeline	20.54	216.1511	218.1386
	cis-Lobelanine/ trans-Lobelanine	20.66	96.0814	216.1378
	cis-Lobelanidine/ trans-Lobelanidine	20.86	218.15442	202.1583
	Norlobelanine	20.89	202.1223	82.0657
	cis-Lobelanine/ trans-Lobelanine	21.15	96.0813	216.138
	Lobinaline	28.49	214.1599	295.0956

Plant	Alkaloid	RT (min)	fragment (m/z) 1	fragment (m/z) 2
Solanum nigrum	beta-Solamargine	21.75	/	/
Senecio vulgaris	Rubbelline / Seneciphylline	9.52	120.0809	138.0901
	Usaramine/ Integerrimine	10.73	94.066	138.0918
	Spartioidine	11.39	120.0803	138.0919
	Senecionine/ Integerrimine	12.63	120.0815	138.0919
	Usaramine/ Integerrimine	14.05	94.0652	120.0805
Datura stramonium	Tropinone	14.08	108.0441	126.05507
	3-acetyltropine	3.79	107.95994	78.88
	3,6-diacetyltropine	3.86	110.0599	71.0494
	Apohyoscyamine	17.88	/	/
Veratrum album	Cevadine	17.17	574.3358	556.3259
	Cevadine	18.07	574.3346	474.2847
	Pseudojervine	18.54	526.849	188.4952
Plantago major	Indicain	5.8	/	/
	Plantagonin	4.36	/	/
Ranunculus montanus	Magnoflorine	15.04	297.114	265.0847
Arnica montana	2-Pirrolidinoacetic acid	3.51	70.0652	112.0866
Valeriana officinalis	Actinidine	13.0	130.0861	120.0196
	Valerine	5.2	96.0810	122.0965
	Cathinine	5.26	132.1018	135.0677
	Valerianine	8.92	134.0969	119.0730
	Valerianine	12.95	118.0731	146.0959
Cinchona succirubra	Cinchoranine F	12.0	253.1527	261.1643
	Cinchoranine C	14.8	293.1642	138.1119
	Cinchoranine E	15.7	277.1693	
	Cinchoranine G	16.0	309.1955	160.0755
	Cinchoranine C	16.3	293.1641	130.0649
	Cinchoranine F	19.0	309.1953	184.0754
	Cinchoranine B	19.5	138.1116	121.0885
	Cinchoranine B	23.4	121.0884	184.0733

Figure 1

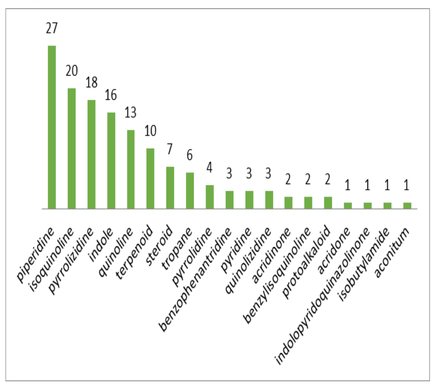

Figure 2

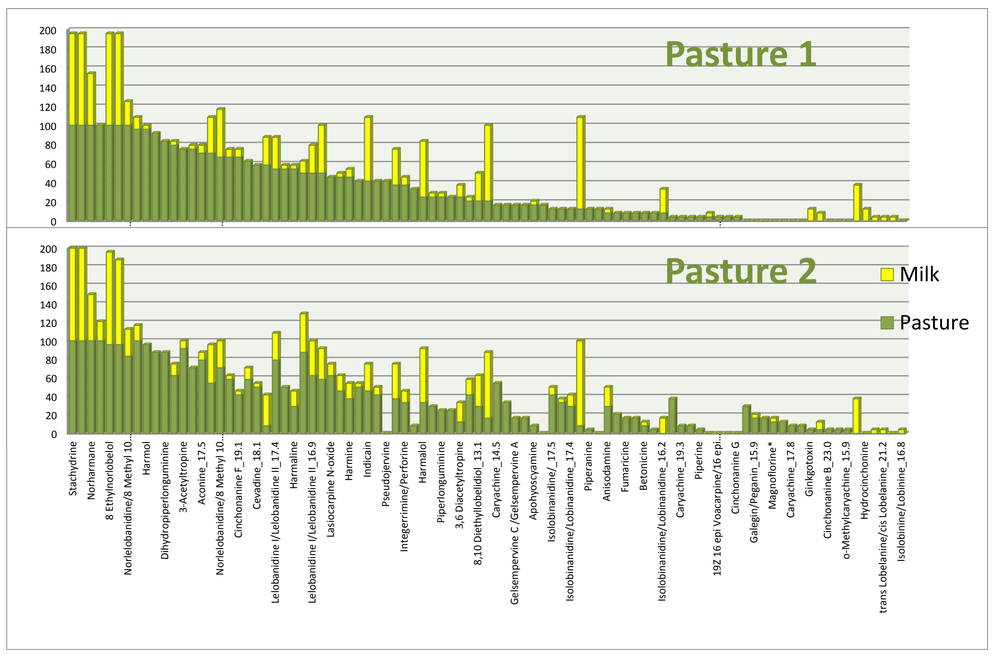

Table 2

Compound	Nicotine	Monocrotaline	Lycopsamine	Coniine	Erucifoline	Senecionine N-oxide	Gramine	Theobromine/ Theophylline	Scopolamine	Jacobine-N-oxide	Erucifoline-N-oxide	Heliotrine	Retrorsine	Seneciphylline	Retrorsine N-oxide	Senecionine/ Seneciverrine	Hyoscyamine/ Atropine	Echimidine	Senkirkin	Jacobine	Caffeine	Lasiocarpine	Strikoline	Harmaline	Sipeimine	Quinine	Quinidine	Veratramine	alpha-Solasonine	Jervine	alpha-Solamargine	Protoveratrine A	Veratridine	alpha-Solanine	Solasodine	Aconitine	Tomatidine/ Tomatine
RT (min)	4.73	5.25	6.96	7.59	8.44	8.97	9.28	9.57	10.25	10.52	10.66	10.71	10.73	11.4	11.89	12.63	12.65	13.64	13.94	14.05	15.09	15.8	16.33	16.42	17.55	18.3	18.82	19.68	19.83	19.85	20	20.62	21.65	21.77	23.6	23.68	24.54
LOD (µg L^{-1})	15	0.05	0.12	0.21	0.07	0.05	0.05	2.8	0.2	0.28	0.35	0.04	0.25	0.14	0.43	0.14	0.15	0.08	0.66	0.28	0.92	0.12	0.59	3.49	1.18	1.95	2.9	0.18	0.1	0.26	2.73	10.7	0.14	1.28	0.65	1.24	5.99
LOQ (µg L^{-1})	50	0.17	0.4	0.71	0.25	0.17	0.16	9.3	0.65	0.94	1.18	0.14	0.83	0.56	1.43	0.46	0.51	0.25	2.22	0.95	3.06	0.41	1.86	11.6	3.92	6.5	9.7	0.59	0.35	0.86	9.1	35.7	0.45	4.26	2.16	4.12	20
Linearity range (µg L-1)	50-4000	0.17-1000	0.40-1000	0.71-1000	0.25-1000	0.17-1000	0.16-1500	9.3-500	0.65-2000	0.94-1500	1.18-1000	0.14-1000	0.83-1500	0.58-2000	1.43-1500	0.46-1500	0.51-2000	0.25-500	2.22-1000	0.95-1500	3.06-500	0.41-1500	1.86-1500	11.63-3000	3.92-1000	6.5-200	9.7-500	0.59-1000	0.25-1000	0.86-2000	0.11-1500	35.71-1500	0.45-1500	4.26-500	2.16-1000	4.12-1500	19.97-3000
R^2	0.99	0.998	0.998	0.998	0.998	0.997	0.998	0.999	0.996	0.996	0.996	0.998	0.996	0.996	0.996	0.993	0.994	0.999	0.998	0.997	0.998	0.998	0.993	0.996	0.998	0.996	0.995	0.995	1,000	0.995	0.999	0.996	0.998	0.998	0.993	0.999	0.991

Dott.ssa Tiziana Nardin
Prof. Edi Piasentier
Prof. Roberto Larcher

Info:
Tel. +39 0461 615119
Fax. +39 0461 615288
Indirizzo mail tiziana.nardin@fmach.it

Riferimenti bibliografici

[1] M. Yanga, J. Sunb, Z. Lua, G. Chena, S. Guana, X. Liua, B. Jianga, M. Ye, De-An Guo, Journal of Chromatography A, 1216, 2045–2062 (2009).
[2] T. Nardin, E. Piasentier, C. Barnaba, R. Larcher, Journal of Mass Spectrometry, 51(9):729-41 (2016).
[3] T. Nardin, E. Piasentier, C. Barnaba, R. Larcher, Food Chemistry, submetted (2017).

UNIVERSITÀ DEGLI STUDI DI UDINE
hic sunt futura

LIFE SCIENCES
30° ciclo
Corso di dottorato in Scienze e biotecnologie agrarie

Rumen utilization of urea-based feeds by in vitro studies.

Introduction

Bacteria inhabiting the rumen convert ammonia-nitrogen from NPN (such as urea) into high-quality microbial protein, which is the key to ruminant productivity (Nikulina et al., 2017; Spanghero et al., 2017). Yet, the high degradation rate of urea in the rumen normally exceeds the ability of bacteria to catch the ammonia released due to the relatively slower energy supply from carbohydrates degradation. Slow-release urea (SRU) provide slow and continuous N supply for optimal microbial protein synthesis. The SRU products are generally tested by direct incubation in the rumen, but it requires cannulated animals and is labor expensive. Ethical and economic issue suggest developing alternative methods based on the usage of laboratory techniques (in vitro).

In vitro studies to evaluate the N rumen release

Urea-treated high moisture cereal grains

Present work evaluated the high moisture grains (barley and corn) treated with urea at harvesting, primarily, for the preserving goals. The hypothesis was that during the treatment ammonia binds inside the kernel, resulting in slow-release ammonia effect while digested. Two different rumen in vitro fermentation systems were applied. Ammonia concentration measured in the fermentation liquid at different time points (Cook et al.,2008) did not differ between urea-treated and grains, supplemented with urea, showing no effect of the treatment studied (Graph 1).

This might be explained by the fine milling of the incubated sample. In the a water solubility test (Caprita et al., 2010) on different physical forms (whole, broken and milled) urea-treated grains showed an increasing N release with the lesser particle size (Graph 2).

Microbial protein synthesis (Grings et al., 2005) was significantly higher for the urea-treated grains comparing to grains supplemented with urea before incubation. Likely, that urea treatment had a slow-release ammonia effect which favored a balance between available ammonia and energy in the rumen. More studies are required on this matter.

Slow-release urea products

The second part of this study (in progress) aims to identify an in vitro method more suitable to evaluate SRU products. Gas-test (Menke, et al., 1979; Blummel and Becker, 1997) and filter-bag incubation (Ankom Technology Daisy II) techniques are conducted on different SRU products. We hypothesized that the Gas-test might be a good alternative to the time and labor-consuming gravimetrical methods.

Possible areas of application

In view of the global shortage of protein resources for animal feeds the increase of N rumen efficiency is highly in demand research area.

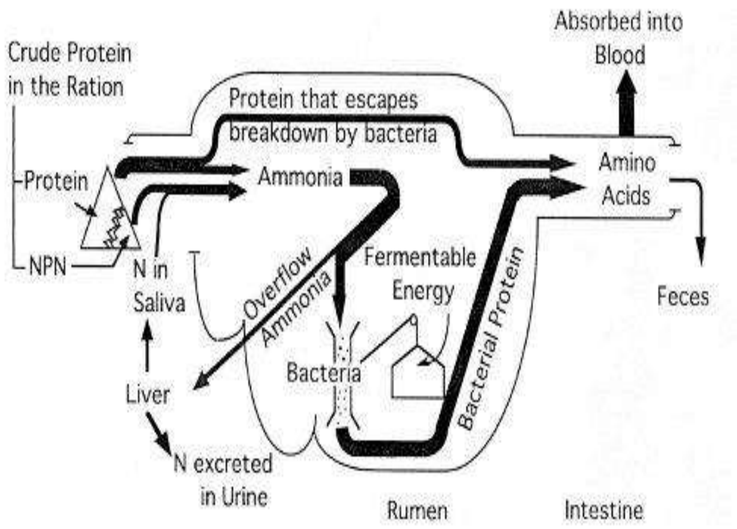

Graph 1

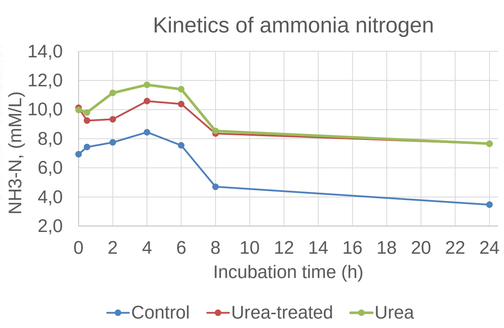

Graph 2

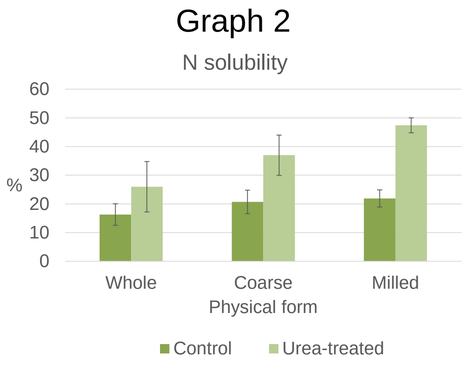

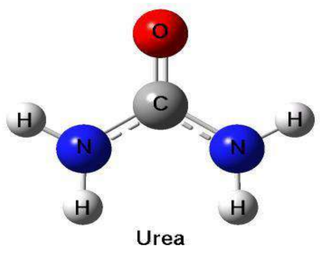

Urea

Dott. Anna Nikulina
Prof. Mauro Spanghero

Info:
Tel. +39 (0432) 558193
E-mails: nikulina.anna@spes.uniud.it.
mauro.spanghero@uniud.it

References

Spanghero, M., Mason, F., Zanfi, C. and Nikulina, A., 2017. Effect of diets differing in protein concentration (low vs medium) and nitrogen source (urea vs soybean meal) on in vitro rumen fermentation and on performance of finishing Italian Simmental bulls. *Livestock Science*, *196*, pp.14-21.

Nikulina, A., Jones, E., Newbold, C.J., Mason, F., Spanghero, M. 2017. Microbial community structure and VFA profile in the rumen liquids from a continuous culture fermenter and in vivo. Poster for the 2nd Congress of the Animal Science and Production Association
.

Acknowledgments

This PhD project is funded by Erasmus Mundus Iamonet Project (2014-2017).

Thanks to the Cost Action DairyCare for the Short Term Scientific Mission to Aberystwyth, the UK, which has promoted international collaboration between laboratories.

UNIVERSITÀ DEGLI STUDI DI UDINE
hic sunt futura

LIFE SCIENCES

30° ciclo

Corso di dottorato in Scienze e biotecnologie agrarie

Next-Generation-Sequencing Metagenomic Analysis of Phytopathogenic Prokaryotes

C. Polano, G. Firrao
Dept. of Agriculture, Food, Environment and Animal Sciences, University of Udine, Via delle Scienze 206, I-33100 Udine, Italy.
Tel: +39 0432 558543 Email: polano.cesare@spes.uniud.it; firrao@uniud.it

In the last fifteen years, DNA sequencing technologies have made fast advancement, through automated optical recognition and reading parallelization, that have allowed *de novo* sequencing of whole genomes with better reliability, shorter times and at a vastly lower cost. The wealth of data made available by these techniques allows more complex numerical analyses and a metagenomic approach to plant endophytes and pathogens population evaluation.

This doctoral project explores four practical applications of this metagenomic approach, aimed to better understand, and possibly help to contrast, pathogens associated to important plant diseases.

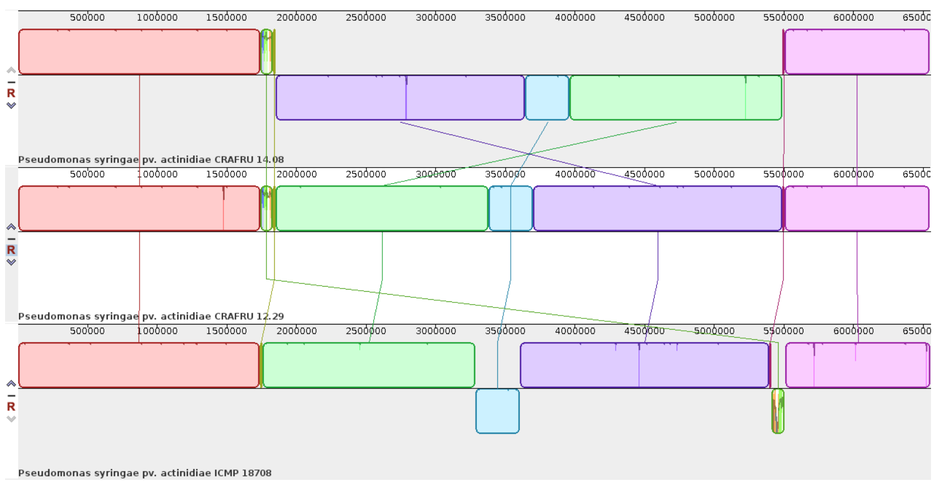

Figure 1. Alignment comparison between two, closely related *Pseudomonas syringae* pv. *actinidiae* strains and a reference genome; note the inversion of half the genome in CRAFRU 14.08 and the transposon in CRAFRU 12.29.

The first one, based on 'third generation' sequencing – capable of producing very long reads and almost gaps-free sequences – intends to determine the genetic basis of the absence of hypersensitive response in tobacco plants[1] to the *Pseudomonas syringae* pv. *actinidiae* strain CRAFRU 12.29, compared to the very close strain CRAFRU 14.08 (fig. 1).

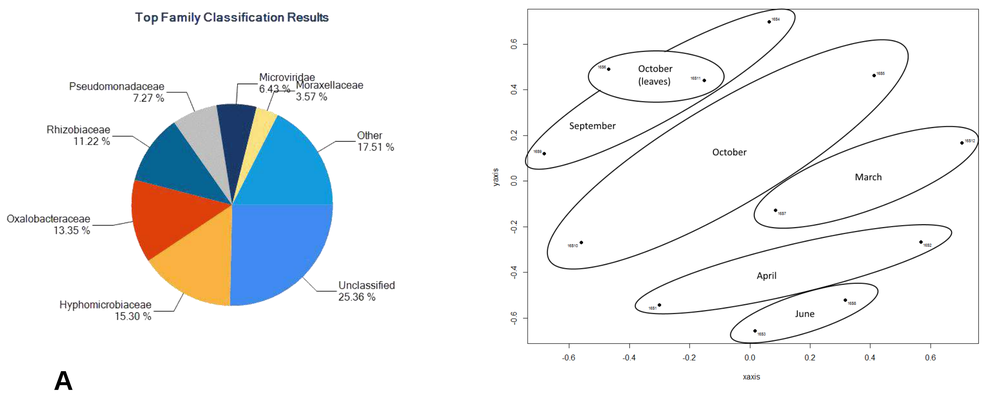

A

Figure 2A. Preliminary classification of the endophyte fauna in kiwifruit samples (courtesy of Illumina, Inc.).

Figure 2B. Draft OTU-based NMDS analysis of the endophyte fauna in kiwifruit.

The second application is the multivariate analysis[2] of endophytes diversity in kiwifruit (fig. 2A and 2B) and their relations with, and possible mitigation of, *Pseudomonas syringae* pv. *actinidiae,* using 16S ribosomal RNA sampled from plant specimens collected at various times during the year.

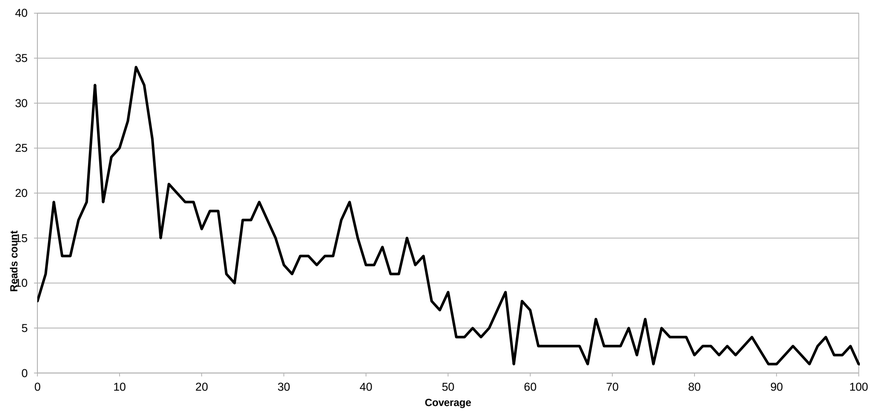

Figure 3. Coverage graph of a Milkweed Yellows phytoplasma infected periwinkle sequencing; the vertical line marks a cutoff value used with *Phytoassembly.*

The third application is the computational reconstruction of the genome of non-colturable, and therefore difficult-to-sequence, pathogens like phytoplasmas from a diseased plant sequencing, using a Bash/BioPerl pipeline (named *Phytoassembly*) and commonly available bioinformatic tools.

The pipeline sets a cutoff point (fig. 3) based on the differential in coverage[3] of the plant and the phytoplasma sequence contigs; the remaining reads are then filtered against a healty plant reference.

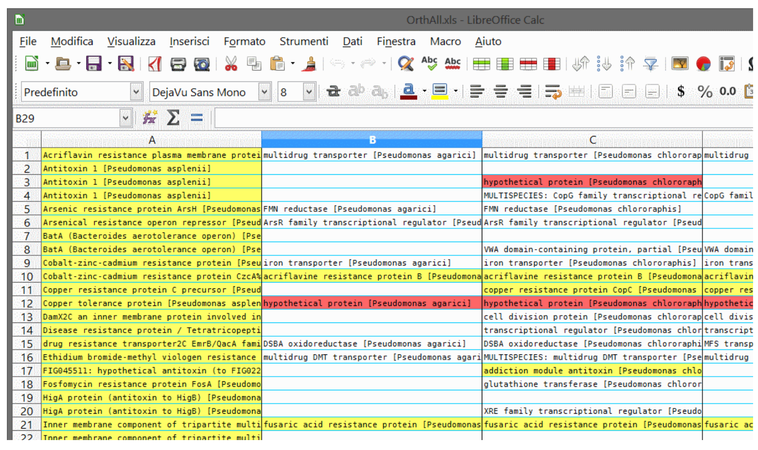

Figure 4. Partial table of the orthologs comparison between a *Pseudomonas asplenii* strain and reference genomes of *P. fuscovaginae* and *P. agarici.*

The fourth application is the annotation and comparative analysis of *Pseudomonas* strains, based principally on the inference of orthologs among genomes (fig. 4).

References
[1] Mazzaglia, A., *et al.* (2012). *Pseudomonas syringae* pv. *actinidiae* (PSA) isolates from recent bacterial canker of kiwifruit outbreaks belong to the same genetic lineage. *PloS One,* 7: e36518.
[2] Ramette, A. (2007). Multivariate analyses in microbial ecology. *FEMS Microbiology Ecology,* 62 (2), 142–160.
[3] Saccardo, F., *et al.* (2012). Genome drafts of four phytoplasma strains of the ribosomal group 16SrIII. *Microbiology,* 158 (Pt_11), 2805–2814.
[4] Altenhoff A et al. (2015). The OMA orthology database in 2015: function predictions, better plant support, synteny view and other improvements. *Nucleic Acids Research,* 43 (D1): D240–D249.

UNIVERSITÀ DEGLI STUDI DI UDINE
hic sunt futura

LIFE SCIENCES

30° ciclo
Corso di dottorato in Scienze e biotecnologie agrarie

Improvement of chemical quality index of wines from interspecific hybrids

Introduction

Recurrent environmental issues related to the high and continuous use of pesticides in order to control the grapevine pathogens have recently stimulated the interest on the production of interspecific hybrids. These hybrids, also called fungus-resistant PIWI varieties, are the result of interspecific crossbreeding between wild American *Vitis* species which carry resistant traits to fungal diseases and European *Vitis vinifera* varieties which show good quality traits.

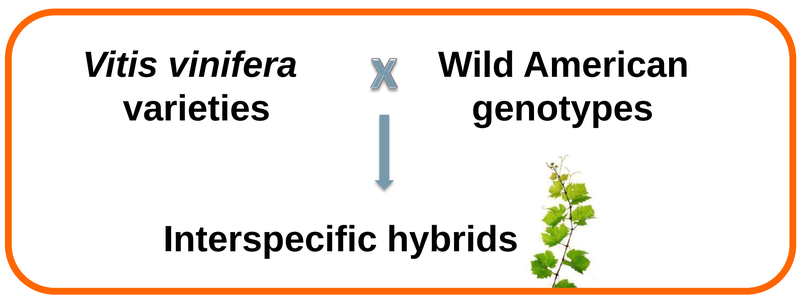

Aim and future perspective

The aim of this project was to investigate the chemical composition of grapes and wines (white and red) obtained from a selection of interspecific hybrids grown in two experimental fields, in Italy and Germany, in three different vintages. The perspective is to produce a comprehensive scientific study to classify the grapes and wines according to their metabolite profile.

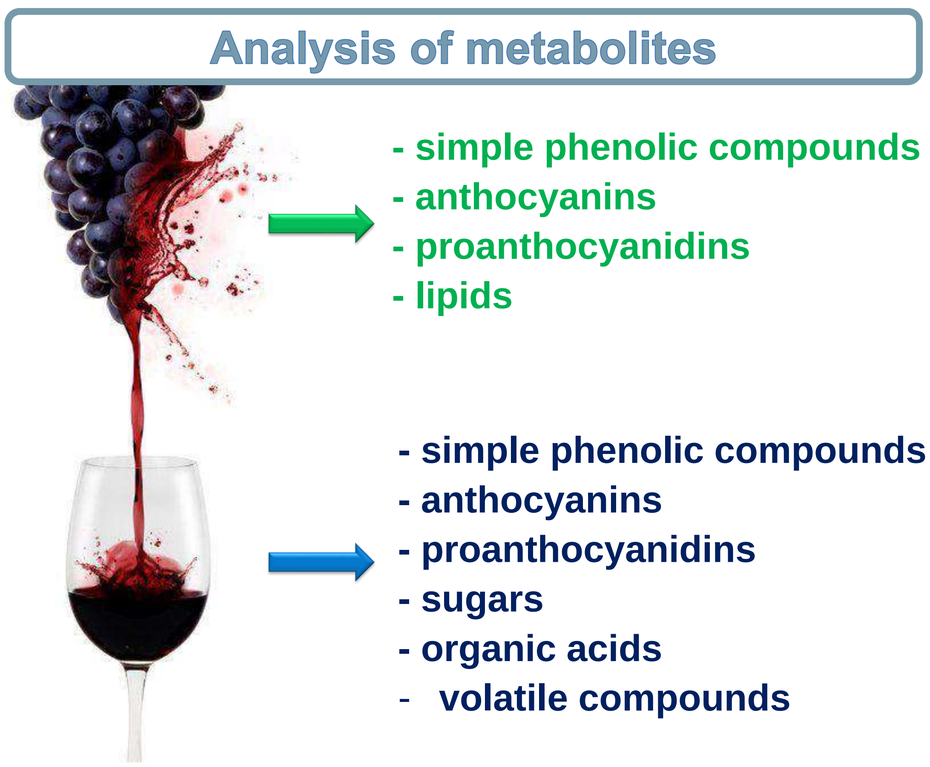

Fig.1 List of the metabolites analysed in grapes and wines.

Diglucosides: markers for interspecific hybrids

Anthocyanins are the main compounds responsible for the color of red grapes and wines. The composition in anthocyanins of interspecific varieties differs from that of *Vitis vinifera* in the presence of 3-5-diglucosides and more specifically malvidin-3-5-diglucoside.

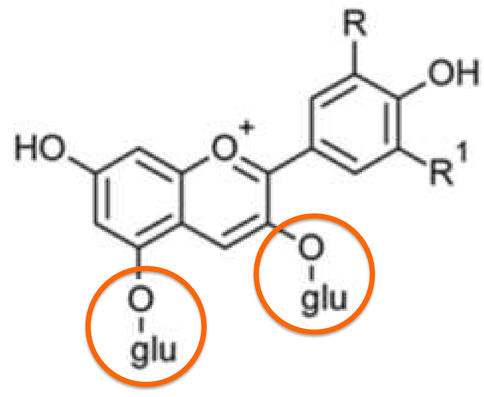

Fig. 2 Chemical structure of malvidin-3,5-diglucoside.

In fact, in *V. vinifera* varieties glycosylation occurs at the 3' position, while in non-*V. vinifera* species it occurs also at the 5' position, resulting in the presence of diglucoside anthocyanins. Although no evidence of any negative influence of these compounds on the quality of the wine and human health has been found, the acceptable limits of anthocyanin diglucosides in wines for the European markets is 15 mg/L.
Therefore, the evaluation of their presence and content in the interspecific hybrids is of particular interest.

Results and discussion

The results showed differences in anthocyanin composition, since diglucosides were found in highly variable amounts in red wines analysed. Multivariate methods were applied to visualize and evaluate similarities and differences in the volatile and non- volatile profile of the interspecific hybrids studied.

Conclusion

This work provides a clear picture of the chemical profile of grapes and wines of the most promising interspecific hybrids. This information allows to identify the most peculiar aspects of their composition, measuring their positive and negative quality traits.
Up to our knowledge this is the most extended profiling study on interspecific hybrids.

Dott. Silvia Ruocco
Prof. Urska Vrhovsek

Info:
Tel. +39 0461615124
ruocco.silvia@spes.uniud.it
urska.vrhovsek@fmach.it

References

- Pedneault K. et al (2016), Sci. Hortic., 208: 57–77
- Ruocco S. et al. (2017), Food Res. Int.
- J. A. Considine, E. Frankish. A Complete Guide to Quality in Small-Scale Wine Making. Elsevier Inc.: Kidlington, Oxford, 2014.

Acknowledgements

This work was financially supported by the ADP project, funded by the Autonomous Province of Trento, Italy.

UNIVERSITÀ DEGLI STUDI DI UDINE
hic sunt futura

LIFE SCIENCES
30° ciclo
Corso di dottorato in Scienze e biotecnologie agrarie

Grapevine pest management through natural compounds and agronomic practices

Lotta contro i fitofagi della vite con sostanze di origine naturale e pratiche agronomiche

Dott. Federico Tacoli, Prof. Francesco Pavan
Info: Tel. +39 0432 558508 E-mail: tacoli.federico@spes.uniud.it, francesco.pavan@uniud.it

Introduction
In the context of integrated pest management, the substitution of chemical control with alternative sustainable tools is the main focus in Europe (Directive 128/2009/EC). During this PhD we investigated the effects of bunch-zone leaf removal and natural compounds in controlling grapevine pests, such as the European grapevine moth *Lobesia botrana*, the leafhoppers *Empoasca vitis* and *Zygina rhamni* and the grapevines' mealybug *Planococcus ficus*. We also considered the side effects on natural enemies and non-target arthropods.

Effects of bunch-zone leaf removal.
Bunch-zone leaf removal is usually applied, either manually or mechanically, from pre-bloom to veraison to control bunch rots. The reduction of the leaf density decreases humidity in the canopy and exposes bunches to sunlight.
In our studies bunch-zone leaf removal reduced *L. botrana* infestation by 40% (Fig. 1) but did not influence grapevine leafhoppers. This practice slightly reduced the number of predatory mites (Phytoseiidae) and Salticidae spiders, while increased the number of ladybirds and predatory Thysanoptera. These outcomes suggest that bunch-zone leaf removal can be used to reduce insecticide input for the control of *L. botrana* in vineyards without significant interference with biological control.

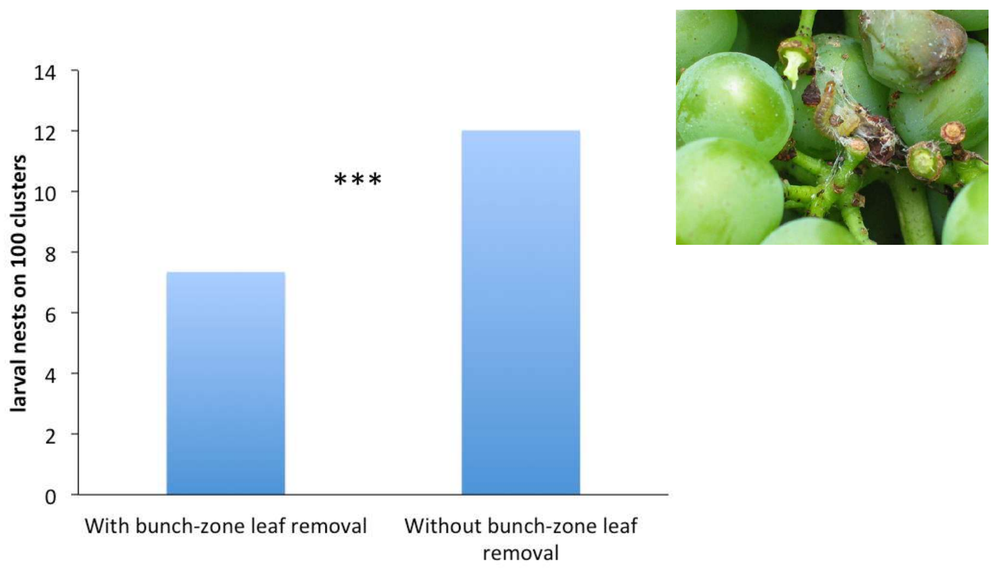

Fig. 1 – Effect of bunch-zone leaf removal on *Lobesia botrana.*

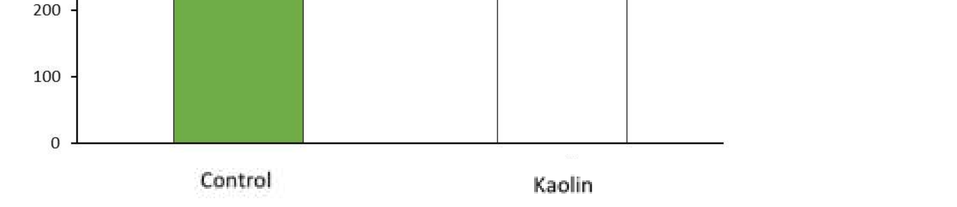

Fig. 2 – Effect of kaolin on *Lobesia botrana* egg-laying in laboratory conditions.

Effects of natural compounds.
We evaluated the effects of kaolin and sulphur powder on *L. botrana*, of kaolin on grapevine leafhoppers and of kaolin and citrus essential oil on the mealybug *P. ficus*, both in laboratory and in field conditions.
In laboratory conditions kaolin and sulphur powder were able to reduce the number of eggs laid by *L. botrana* (Fig. 2) and egg-hatching rate. Kaolin also acted as a repellent for both adults and larvae, these last effects have not yet been investigated for sulphur powder. Studies about the effects in field conditions are still ongoing.
In both laboratory and field conditions kaolin affected grapevine leafhoppers feeding behavior, leafhoppers did not feed on leaves sprayed with kaolin and then died due to desiccation. In field trials kaolin had the same efficacy of commercial insecticides when applied before the infestation had started (Fig. 3).
In both laboratory and field conditions kaolin was not effective in controlling *P. ficus*, whereas citrus essential oil was able to control the mealybug reducing the infestation level in field conditions by 58% (Fig. 4).
Kaolin reduced the numbers of predatory mites (Phytoseiidae) during the summer. However, overwintering populations were not affected and in the subsequent year mite numbers were not different from the control. Kaolin slightly reduced also spiders but other arthropods were not affected.
These outcomes suggest that kaolin can be used to control grapevines' leafhoppers in vineyards with minimal detrimental effects on natural enemies. This compound together with sulphur powder could be of valuable use for the control of *L. botrana* but not against *P. ficus*, for which citrus essential oil could be an alternative to insecticides.

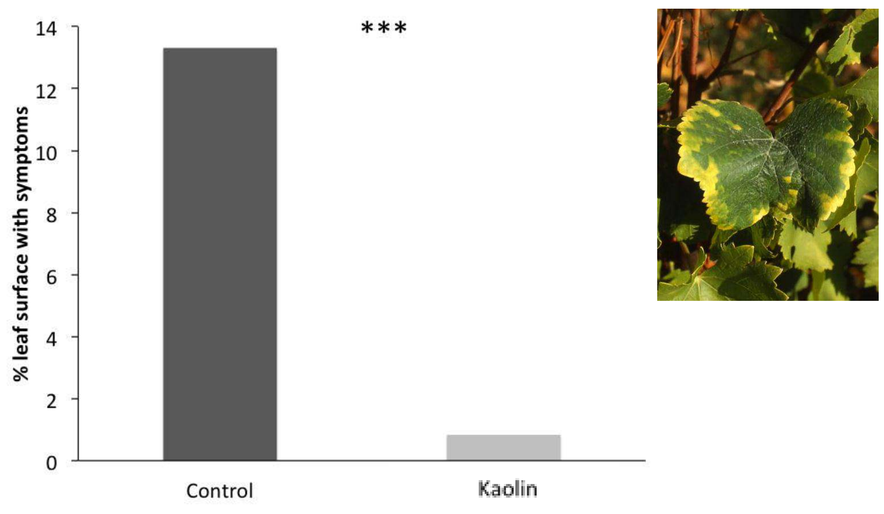

Fig. 3 – Effect of kaolin on grapevine leafhoppers damage in field conditions.

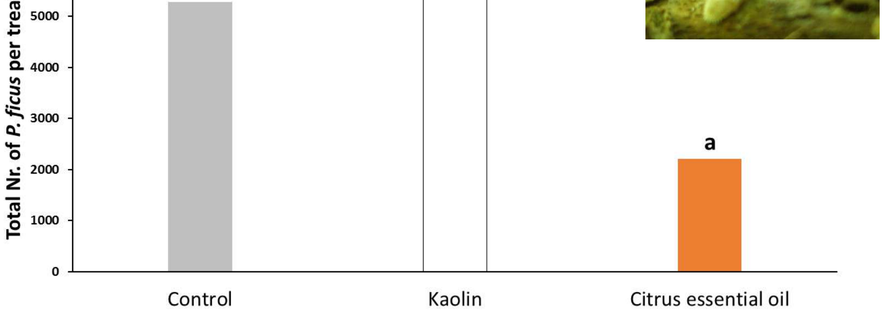

Fig. 4 – Effect of kaolin and citrus essential oil on grapevine mealybugs infestation in field conditions.

UNIVERSITÀ DEGLI STUDI DI UDINE
hic sunt futura

LIFE SCIENCES

30° ciclo
Corso di dottorato in Scienze e biotecnologie agrarie

Il benessere della bovina da latte: un'opportunità per produttori e consumatori

Il benessere animale come attributo di qualità

Il benessere animale è considerato un aspetto di crescente interesse per il consumatore e di conseguenza ha velocemente trovato posto nell'agenda politica europea e nazionale.

La metodologia di valutazione

Nel settore delle vacche da latte non esistono normative specifiche per il monitoraggio del benessere animale a livello aziendale. Nel 2015, il Centro di Referenza Nazionale per il Benessere Animale (CReNBA) ha depositato a livello ministeriale il primo protocollo per la valutazione del benessere delle vacche da latte. Nello stesso anno, l'Agenzia Europea per la Sicurezza Alimentare (EFSA, 2015) ha sviluppato un protocollo basato sul progetto Welfare Quality®, ma semplificato per le aziende di piccola scala (< 75 capi adulti). Questa tipologia aziendale è preponderante non solo a livello europeo ma anche a livello nazionale ed in particolare nelle zone di montagna (Zuliani et al., 2017).

Lo studio ha avuto come primo obiettivo quello di applicare il protocollo EFSA in un campione di aziende montane della regione Alpe Adria (Friuli, Veneto, Trentino-Alto Adige, Austria e Slovenia) al fine di valutare la sua fattibilità in condizioni di pascolo e stalla e di proporre uno strumento di monitoraggio del benessere animale tarato sulla realtà locale.

La comunicazione al consumatore

La seconda fase del progetto ha l'obiettivo di valutare l'interesse del consumatore nei riguardi di informazioni relative al benessere animale quando aggiunte in etichetta. Gruppi di consumatori, reclutati sia a livello urbano sia rurale, verranno invitati da un moderatore a discutere delle prerogative dell' agricoltura di montagna, del benessere animale e delle preferenze comunicative in etichetta.

Gli indicatori di benessere nelle aziende di vacche da latte di piccola scala

Principi	Criteri	Indicatori
Buona alimentazione	Assenza di fame	Condizione corporea
	Assenza di sete	Abbeveratoi funzionanti e puliti
Buona stabulazione	Comfort in cuccetta	Movimento di alzata Pulizia dell'animale
	Libertà di movimento	Presenza di posta fissa/libera Accesso al pascolo (h/d)
Buona salute	Assenza di lesioni	Presenza di aree alopeciche Presenza di lesioni aperte e gonfiori, Presenza di zoppie Condizione degli unghioni
	Assenza di segni clinici di malattia	Presenza di scoli oculari, nasali, vaginali Respirazione difficoltosa Mastiti, Vacche a terra Parti difficili Mortalità Longevità
	Assenza di dolore indotto	Decornazione Cow-trainer
Comportamento naturale	Relazione uomo-animale	Distanza di fuga
	Stato emotivo	Valutazione del comportamento (intera mandria)

Prospettive

Il monitoraggio del benessere animale con protocolli adatti alle realtà di allevamento locale, l'individuazione di criticità e lo sviluppo di azioni volte al loro superamento associati ad una comunicazione semplice ma corretta al consumatore possono essere strumenti fondamentali per accrescere il valore aggiunto dei prodotti lattiero-caseari locali, promuovendo filiere etiche e trasparenti.

MONITORARE

COMUNICARE

Contatti

Dott.ssa **Anna Zuliani**
Prof. **Stefano Bovolenta**

Tel. +39 0432 558177
E-mail zuliani.anna.2@spes.uniud.it

Riferimenti bibliografici

EFSA AHWA Panel 2015 Scientific Opinion on the assessment of dairy cow welfare in small-scale farming systems. *EFSA Journal* 13, 4137-4239

Zuliani A., Romanzin A., Corazzin, M.; Salvador, S.; Abrahantes, J.C.; Bovolenta, S 2017. Welfare assessment in traditional mountain dairy farms: above and beyond resource-based measures. *Animal Welfare*. 26, 203-211

Welfare Quality® 2009 Welfare Quality® assessment protocol for cattle. Welfare Quality Consortium. Lelystad, Netherlands

UNIVERSITÀ DEGLI STUDI DI UDINE
hic sunt futura

LIFE SCIENCES

30° ciclo

Corso di dottorato in Scienze e biotecnologie agrarie

Oxidative metabolism during wheelchair propulsion tests in patients with spinal cord injury: effects of lesion level

Biasutti, L.[1], Blanco, R.[2], Floreani, M.[1], Bizzarini, E.[2], Grassi, B.[1]
[1] University of Udine, [2] IMFR Gervasutta, Udine

BACKGROUND

Spinal cord injuries (SCI) lead to impairments in lower and/or upper limbs movements as well as several other physiological aspects such as metabolism, cardiovascular system, neuromuscolar system, thermoregulation etc. The lesion level and the completeness of the lesion, are determining factor for the variance in physical capacity in SCI patients. Furthermore, the efficiency of wheelchair propulsion has been shown to be very low if compared with other forms of upper body locomotion (arm-cranking, hand-cycling), and few studies have been performed using everyday wheelchair. Moreover, the knowledge of wheelchair propulsion effects on able bodied could be of interest also for potential effects for person with other disabilities.

METHODS

A functional evaluation of oxidative metabolism during exercise was carried out on 16 patients with spinal cord injury (SCI): 9 paraplegic (P, lesion level D4-D12, BMI 22.67 ±2.33, age 36± 7.60 yr.) and 7 tetraplegic (T, lesion level C4-C8, BMI 21.05 ±2.9, age 40.14 ±9.6 yr.) were tested 14.87 ±9.33 yr. after the event (n=15 traumatic, n=2 non-traumatic). Two 4-min exercises were performed on a computer-controlled ergometer (with no resistance set on rollers) in the patient's everyday wheelchair, one at the self-selected speed (SSS), and one at the maximal sustainable speed during an "all-out" effort (MS). Seven able-bodied control subjects (CTRL, BMI 23.28 ±2.83, age 33 ±10.79 yr.) performed 3 exercises: one a T mean speed, one at P mean speed and one at their own maximal sustainable speed. Pulmonary O_2 uptake ($V'O_2$), energy cost of wheelchair propulsion (C), heart rate (HR), push frequency and push efficiency (i.e. distance per push) were determined. Furthermore, muscle recruitment patterns by EMG and biomechanical analyses have been performed.

Fig. 1-2
Test and equipment set up.

RESULTS

Mean values of $V'O_2$, HR, velocity and push frequency during 4' MS were inversely and linearly correlated with the lesion level, and were higher in P and CTRL vs T. Contrarily, no correlation to lesion level was found for C values and push efficiency.
Similarly, $V'O_{2peak}$ was higher in P (1.50 ± 0.49 l/min) and CTRL (1.66 ±0.49 l/min) vs. T (0.72 ± 0.27 l/min). Thus, HR_{peak} corresponded to 117.5 ±25.36 and 161.28 ±12.72 b/min, respectively, in T and in P and to 162.18 ±12.10 b/min in CTRL, being again significantly lower in T vs. P and CTRL.
Interestingly, if compared at same velocity, no differences were found for any variable between SCI and CTRL subjects. Likewise, no differences between T and P were observed during 4' SSS.
In conclusion, a higher level of lesion in people with SCI was found to be associated with a lower performance, likely due to cardiovascular and muscle recruitment limitations. Nevertheless, push efficiency and O_2 cost of pushing were found to be similar in both patients groups as well as CTRL. Further insights could be gained from the EMG and kinematic analysis in relation to metabolic parameters.

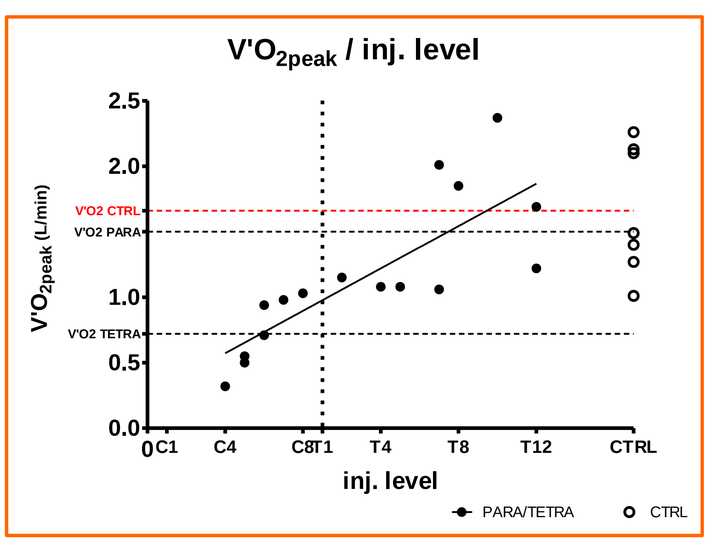

Fig. 3 $V'O_{2peak}$ at MS in T, P and CTRL subjects

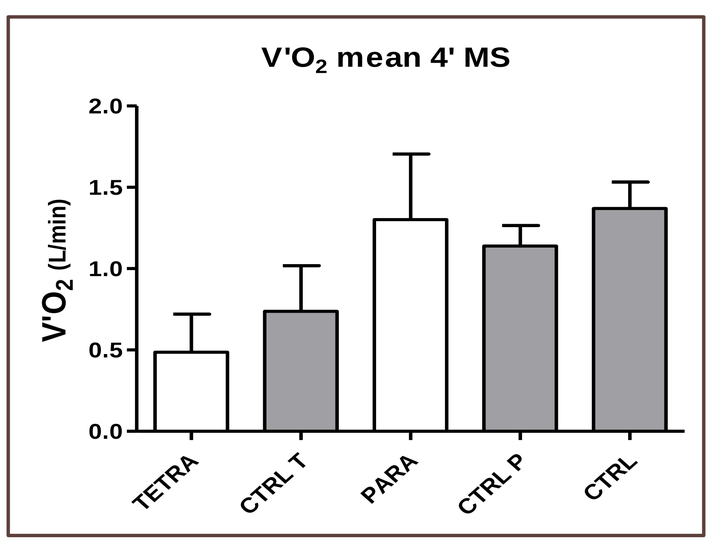

Fig. 4 $V'O_{2mean}$ at MS in T, P and CTRL compared at same VEL

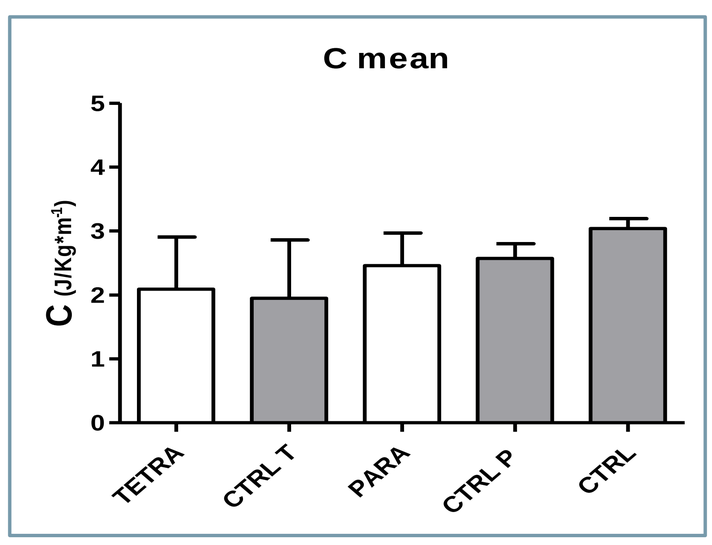

Fig. 5 C_{mean} at MS in T, P and CTRL compared at same VEL

Dott.ssa Lea Biasutti
Prof. Bruno Grassi

Department of Medical Area
Tel +39 0432 494330
Email biasutti.lea@spes.uniud.it
Email bruno.grassi@uniud.it

BIBLIOGRAPHY

Efficiency of Wheelchair Propulsion and Effects of Strategy, *Lenton JP et al, 2008*
Normative values and determinants of physical capacity in individuals with spinal cord injury, *Thomas W.J. Janssen et al., 2002*
Exercise training programs to improve hand rim wheelchair propulsion capacity: a systematic review, *Zwinkels M et al., 2014*

ACKNOWLEDGEMENTS
Istituto di Medicina Fisica e Riabilitazione "Gervasutta", Udine

UNIVERSITÀ DEGLI STUDI DI UDINE
hic sunt futura

LIFE SCIENCES

30° ciclo
Corso di dottorato in Scienze biomediche e biotecnologiche

Citrate-stabilized gold nanoparticles hinder fibrillogenesis of a pathological variant of β2-microglobulin

Introduction

The origin of many serious diseases, like Alzheimer's and Parkinson's diseases, have been shown to be related to protein fibrillation into deposits of amyloid aggregates.[1] It has been reported that nanoparticles (NPs) can interact with amyloidogenic proteins and affect their fibrillogenesis.[2] The particular effect in terms of inhibition or promotion seems to depend both on the physicochemical properties of the NPs and the protein nature. Despite the understanding of the detailed mechanism through which nanoparticles interact with amyloidogenic proteins is still challenging, NPs are considered promising and powerful tools for future strategies aimed at the control of fibrillation processes.

Purpose and Methods

We have investigated the effect of citrate stabilized gold nanoparticles (Cit-AuNPs), a simple and versatile kind of NPs widely used in biomedical research,[3] on β2-microglobulin (β2m) which is a paradigmatic amyloidogenic protein, responsible for dialysis related amyloidosis (DRA).[4] Nuclear magnetic resonance (NMR) experiments and molecular dynamic simulations have already shown that the protein preserves its globular native-like structure upon interaction with Cit-AuNPs and the protein is engaged with a preferential interaction patch located at the N-terminal apical part.[5] To investigate the influence of Cit-AuNPs on the fibrillation of β2m, a naturally occurring β2m mutant, D76N, which is responsible for an aggressive systemic amyloidosis[6] and fibrillates at neutral pH, was used.

The fibril formation was analysed at different incubation times through three methods: thioflavin T (ThT) fluorescence, whose intensity increases upon binding with highly ordered amyloid structure proportionally with fibril concentration,[7] transmission electron microscopy (TEM) and native agarose gel electrophoresis.

Results and Discussion

The lower ThT fluorescence and the substantially reduced amount of fibrils detected by TEM when the fibrillogenesis is induced in the presence of Cit-AuNPs suggest that Cit-AuNPs are able to partially hamper D76N β2m fibrillogenesis. Considering that the inhibitory capability decreases as the protein concentration increases and a comparable precipitation kinetics is observed in the absence and in the presence of Cit-AuNPs, the inhibition seems to be due to an effective interaction between Cit-AuNPs and the protein which competes with early stages of aggregation such as protofibril recruitment. Our findings support the occurrence of an interference of Cit-AuNPs along the pathway that leads to D76N β2m fibrillogenesis. This result opens new perspectives for tuning amyloidogenic processes undergone by proteins with properly suited NPs. Understanding the physicochemical mechanisms through which NPs can enhance or supress fibrillogenesis will improve the scientific knowledge of the molecular aspects underlying the amyloid transition that are still poorly understood. Our results are encouraging and support further investigation into nanoparticle-based therapeutic approches for amyloid diseases so far lacking proper treatments.

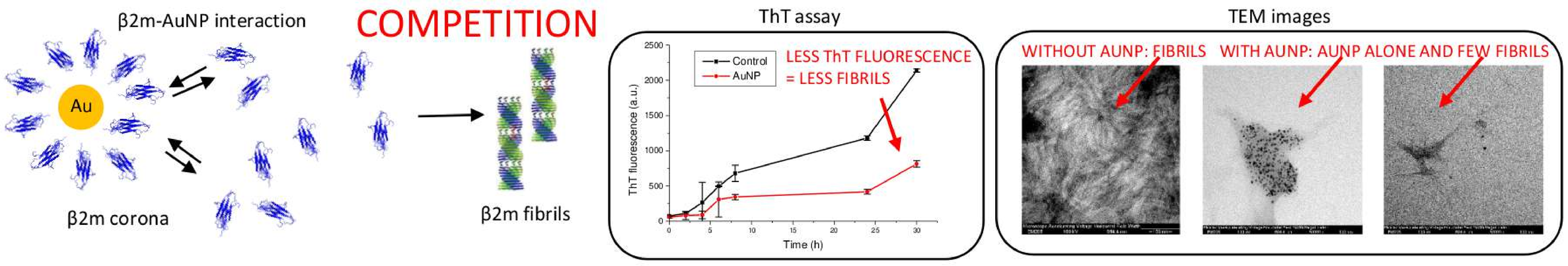

Dott. Cristina Cantarutti
Prof. Gennaro Esposito

Info:
Tel. +39 0432 494325
cantarutti.cristina@spes.uniud.it
gennaro.esposito@uniud.it

References

1) Hardy, J. et al. Science, 2002, 297, 353.
2) Mahmoudi, M. et al. Nanoscale, 2013, 5, 2570.
3) Giljohann, D. A. et al. Angew. Chem. Int. Ed., 2010, 49, 3280.
4) Geyjo, F. et al. Biochem. Biophys. Res. Commun., 1985, 129, 701.
5) Brancolini, G. et al. ACS Nano, 2015, 9, 2600.
6) Valleix, S, M. et al. Engl. J. Med. 2012, 366, 2276.
7) Groenning, M. J. Chem. Biol. 2010, 3, 1.

Aknowledgements

We would like to thank Dr. Sara Raimondi and Sofia Giorgetti from University of Pavia and Dr. Bertoncin Paolo from University of Trieste.

UNIVERSITÀ DEGLI STUDI DI UDINE
hic sunt futura

LIFE SCIENCES

30° ciclo
Corso di dottorato in Scienze biomediche e biotecnologiche

Investigating the role of HDAC7 in the control of mammary gland morphogenesis and transformation

Introduction:

Breast cancer represents the most common cancer in women, but it can also appear in men. Mammary morphogenesis is supervised by the presence of several different instructive signals, which provide the correct gene expression network to generate the proper glandular architecture. These structures transit from a disorganized state to an ordered epithelial organization that modulates polarity, proliferation and luminal cells clearance. Mammary epithelial MCF10A cells cultured on a reconstituted extracellular matrix undergo a morphogenetic process that resembles events found in vivo. MCF10A cells can generate acinar-like spheroids and for this reason they represent one of the best cellular model to study the mammary epithelial morphogenesis.

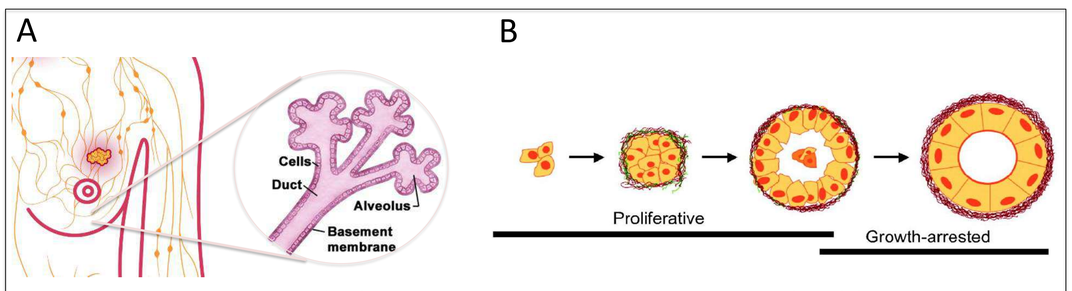

Mammary gland tissue structure and MCF10A as experimental model

A) Schematic rappresentation of a breast tumor and the basic components of a mature mammary gland.
B) Rappresentation of the MCF10A cells morphogenetic process in vitro, through 16 days of culture on a reconstituted extracellular matrix.

Using MCF10A cells as experimental model, we want to investigate the role of the class IIa HDACs (Histone Deacetylases) in breast cancer. In particular, it has been published that HDAC7 is involved in mammary epithelial cells proliferation, through MEF2 (Myocyte Enhancer Factor 2) repression. Indeed, HDAC7 overexpression in MCF10A cells has a pro-growth effect during acini morphogenesis in 3D culture model. Acini, generated in MCF10A cells, engineered to express an inducible super-repressive version of HDAC7 cells, are bigger than the control, manifesting a larger area and a filled lumen.

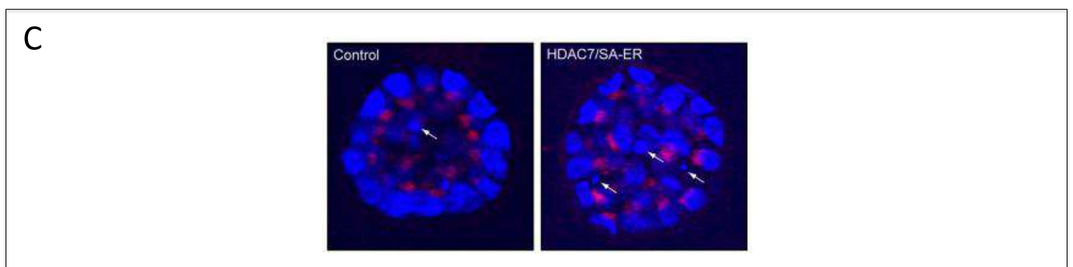

Acinar lumen in MCF10A cells expressing HDAC7 SA-ER

C) Confocal images of MCF10A cells in 3D culture expressing HDAC7/SA-ER vs control.
Picnotic fragmented apoptotic nuclei are shown in the lumen of HDAC7/SA-ER cells acini after 12 days.
Nuclei are stained in Blue and GM130 in red.

Aim of this study:

Exploring the role of HDAC7 in mammary epithelial morphogenesis and neoplastic transformation using CRISPR/Cas9 technology to knock out HDAC7 in MCF10A cells.

Results and Future perspectives:

To explore the role of HDAC7 in MCF10A cells proliferation, we knocked out HDAC7 using the CRISPR/Cas9 technology. MCF10A HDAC7$^{-/-}$ cells exhibit a low proliferation rate possibly due to the de-repression of MEF2 and the subsequent transcriptional up-regulation of the MEF2-regulated gene p21/CDKN1A. The pro-growth effect of HDAC7 in mammary gland morphogenesis was confirmed in 3D culture where the acini formed by the MCF10A HDAC7$^{-/-}$ cells resulted smaller than the control, in particular after four and eight days of 3D culture.

Our studies emphasize a role of the MEF2-HDAC axis in the control of the mammary epithelial morphogenesis and suggest that HDAC7 stimulates epithelial cell growth. The ability to reproduce this phenotype has been confirmed after the re-expression of HDAC7 in the knocked out clones.

In conclusion our results underscore a contribution of the class IIa HDACs and in particular of HDAC7 in cell proliferation and this could explain an important role of HDAC7 in the mammary gland transformation. In future the inhibition of HDAC7 could represent an interesting therapeutic strategy for the breast cancer treatment.

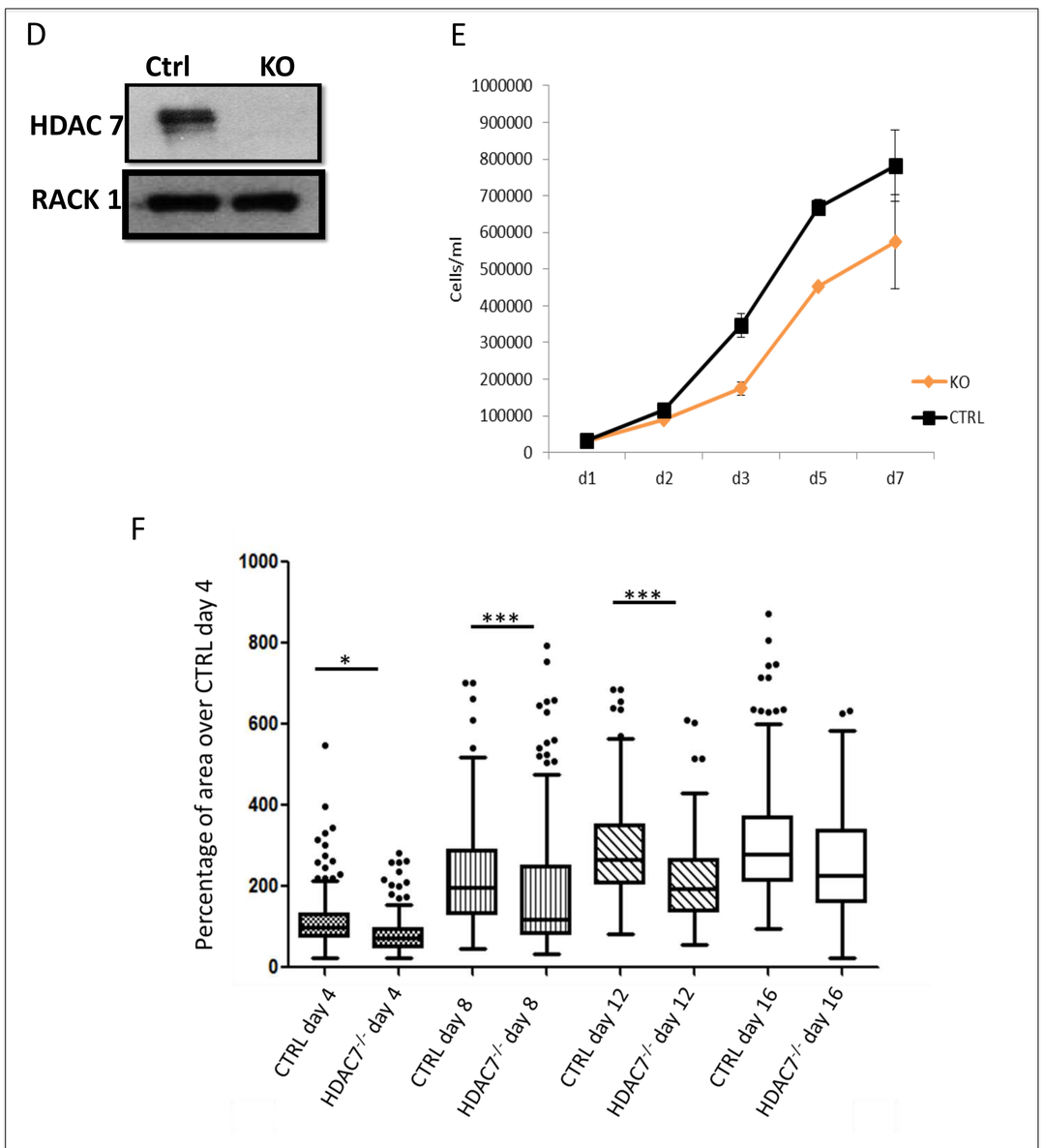

The HDAC7 role in proliferation and epithelial morphogenesis.

D) Immunoblot analysis of HDAC7 levels in MCF10A HDAC7$^{-/-}$ cells and the control. RACK1 was used as loading control.
E) Lower proliferation rate has been observed in MCF10A HDAC7$^{-/-}$ cells compared to the control.
F) Acini resulting from MCF10A HDAC7 KO cells in 3D culture are smaller compared with the control.

Dr. Valentina Cutano
Prof. Cladio Brancolini
Tel. +39 0432494901
cutano.valentina@spes.uniud.it
claudio.brancolini@uniud.it

Bibliography

Clocchiatti et al., JCS 2014
Williams et al., Cancer Res 2008

Acknoledgements

We want to thank A. Clocchiatti (University of Harvard, Boston USA); C. Streuli (University of Manchester UK) S. Cabodi (University of Turin ITALY) AIRC-Associazione Italiana per la ricerca sul Cancro

UNIVERSITÀ DEGLI STUDI DI UDINE
hic sunt futura

LIFE SCIENCES

30° ciclo

Ph.D. course in Biomedical Sciences and Biotechnology

Mast cells during *Candida albicans* infections: new insights for an old player in fungal clearance.

Introduction. *Candida* species are commensal fungi which colonize mucous membranes of healthy individuals. However, they can cause severe invasive disease when mucosal homeostasis is disrupted and especially during the use of immuno-suppressive and anti-neoplastic agents, or broad-spectrum antibiotics. It is extimated that in European intensive care units *Candida* fungaemia mortality rates can range from 28 to 59%.[1]
Mast cells (MC) are important antennae of the immune system, located particularly in mucosal tissues and are among the first cells to get in contact with the external environment. Due to the broad range of receptors and co-stimulatory molecules expressed, and the wide plethora of soluble mediators released, these cells are able to interact with most of the cells in their tissutal microenvironment and are important players in the manteinance of tissue homeostasis.[2]

Aim of the work. Due to their charachteristics and localisaton, mast cells could play a role during fungal infections. To demonstrate this hypothesis we set-up an *in vitro* model to describe the role of these cells during *Candida albicans* infections.

Methods. MC were obtained from murine bone-marrow progenitors cultured for 6 weeks in the presence of IL-3. Mature MC were stimulated with *C. albicans* yeast or hyphae at different time points. RNA was extracted for qPCR analysis of target genes and culture supernatants were collected for cytokine detection by ELISA. For phagocytosis experiments, murine peritoneal macrophages were stimulated with *C. albicans* in the presence of resting or stimulated MC, and phagocytosis index was evaluated by cytofluorimetric analysis.

Results. Despite not being a professional phagocyte, MC can tighly interact with *Candida* and are able to phagocytose the fungus [**Fig. A**]. During the fungal challenge MC are able to express and release several cytokines important for fungal clearance (e.g. TNFα, IL-6, and IL-4) as soon as 3h post-infection [**Fig. C-E**]. Moreover, MC can tightly interact with resident macrophages [**Fig. B**] and can affect macrophages phagocytosis ability. In particular, resting MC are able to inhibit macrophage phagocytosis in a cell-cell contact depentent fashion; once MC are activated by *Candida* this phenotype is reverted and macrophage phagocytosis of the fungus in fully restored [**Fig. F**].

Mast cells can phagocyte *Candida* and tightly interact with macrophages.
A: Mast cell (green) phagocytosing a *Candida* hypha (magenta). **B**: Macrophage (red) engulfing a *Candida* hypha (cyan) which was previously phagocytosed by a mast cell (green).

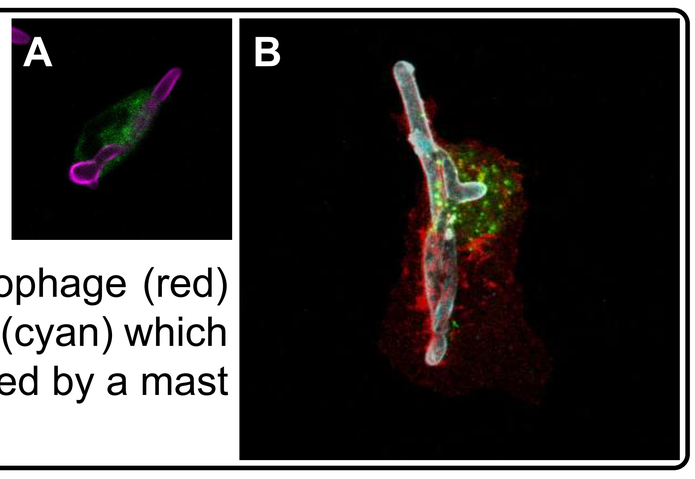

dott. Marco De Zuani
Prof. Carlo E.M. Pucillo
Tel. +39 0432 494342
dezuani.marco@spes.uniud.it

Fundings.
AIRC
Ministero dell'Istruzione
ASIMAS

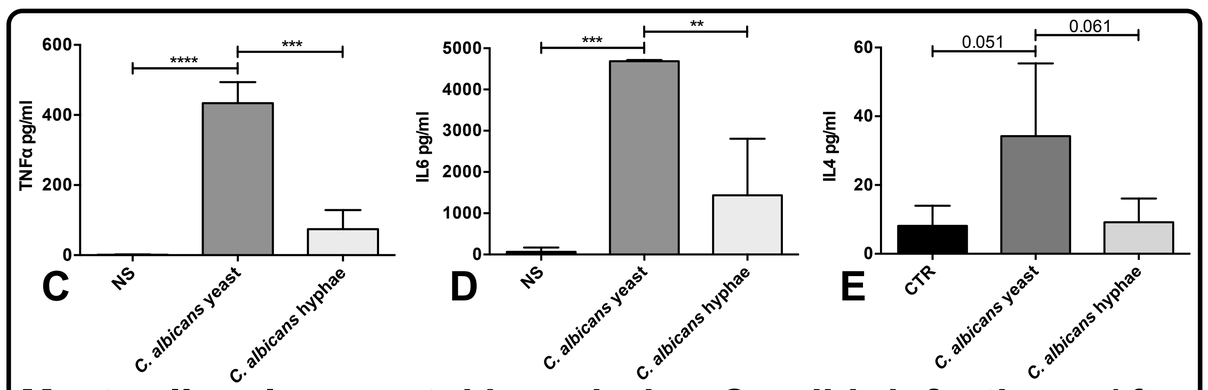

Mast cells release cytokines during *Candida* infections. After infection with *Candida* yeast or hyphae, MC release pro-inflammatory cytokines (TNF-α and IL-6) fundamental for the induction of a prompt antifungal response and IL-4, a Th2 cytokine described to have a fundamental role on the induction of a protective immune response during secondary infections.[3] Data were confirmed also by qPCR analysis of *tnf-α ,il-6* and *il-4* (not shown).

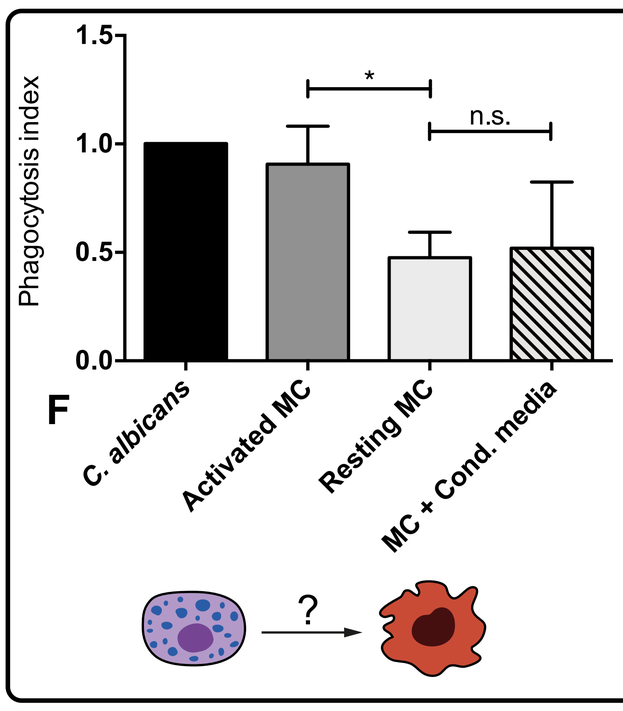

MC activation status affects macrophage phagocytosis of *Candida*. Macrophages stimulated with resting MC show an impaired phagocytosis of *Candida* fungi, while the activation of MC (with Candida yeasts) reverts this phenomenon. Interestingly, this effect is dependent on cell-cell contact as the conditioned media from activated MC fails to revert the normal phagocytosis ability of peritoneal macrophages.

Conclusions. Taken together, these results suggest that MC may play an important role in controlling *Candida* infections by directly interacting with the fungus and limiting fungal growth, and producing cytokines important for fungal clearance. The ability to limit the effector functions of resident macrophages during the initial phase of the infection highlights, once again, that these neglected cells are fundamental players in the maintenance of mucosal homeostasis. Controlling MC activation could be a milestone for novel terapeuthic solutions in the control of *Candida* fungaemia.

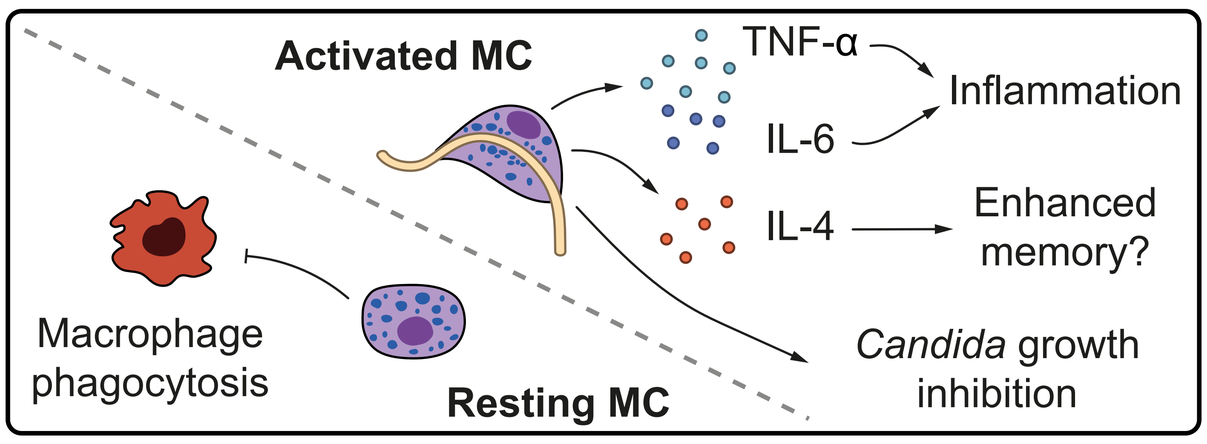

Essential bibliography.
[1] Lass-Flörl, C. (2009). The changing face of epidemiology of invasive fungal disease in Europe. *Mycoses.*
[2] Gri, G et al. (2012). Mast cell: an emerging partner in immune interaction. *Frontiers in immunology.*
[3] Mencacci, A. et al (1998). Endogenous interleukin 4 is required for development of protective CD4⁺ T helper type 1 cell responses to *Candida albicans. J. Exp. Med.*

UNIVERSITÀ DEGLI STUDI DI UDINE
hic sunt futura

LIFE SCIENCES

30° ciclo

Corso di dottorato in Scienze Biomediche e Biotecnologiche

Molecular dynamics simulations of β2-microglobulin interaction with hydrophobic surfaces

Cedrix J. Dongmo Foumthuim, A. Corazza, G. Esposito and F. Fogolari

SIGNIFICANCE

Proteins in their natural cellular environments are considered as a component of a complex solution that may undergo, for either natural or traumatic events, a transition. One such event leading to a metastable condition may be a sudden change of solvation with formation of an aqueous/non aqueous interface, for instance at the boundaries of tissue compartments where interface with lipid membranes occurs. We used molecular dynamics simulations to explore this type of events with β2-microglobulin, a paradigmatic protein model for amyloidogenic pathologies. The results show that β2-microglobulin is readily adsorb to the hydrophobic surface patches and undergoes significant unfolding upon adsorption. Loss of secondary structure and local unfolding could have important physiological consequences suggesting that hydrophobic surfaces could thus act *in vivo* as promoters of partial unfolding and local clustering that are essential for seeding the formation of amyloid fibrils.

RESULTS

Validation of the implicit solvent model used

We checked that the trajectory for 'isolated' proteins was stable on one hand but that also displayed fluctuations similar to those observed in explicit solvent simulations **(Fig.2)**. The per residue fluctuations over all the trajectory for the latters, show that conformational flexibility at the terminal and loop regions were larger **(Fig.3)** and in a range consistent with explicit solvent MD simulations. Overall, the implicit solvent model used wassufficiently accurate to exclude major artifacts in the simulation at least on the timescale considered here.

Fig.2

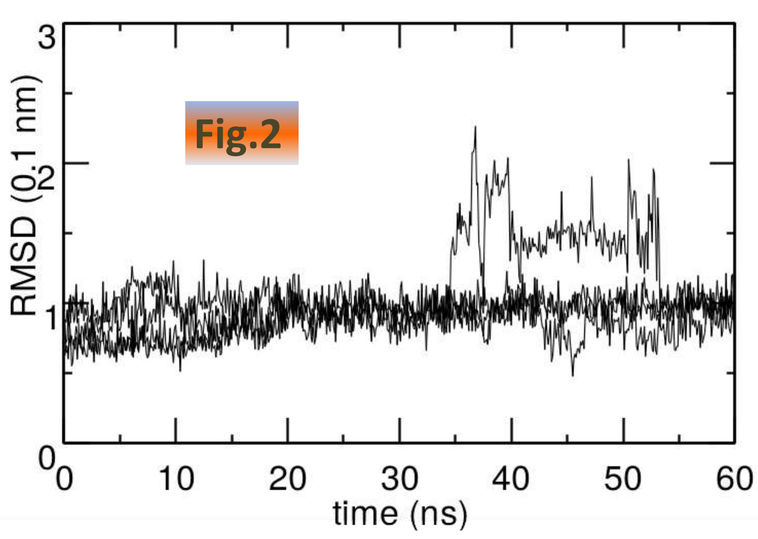

Fig.3

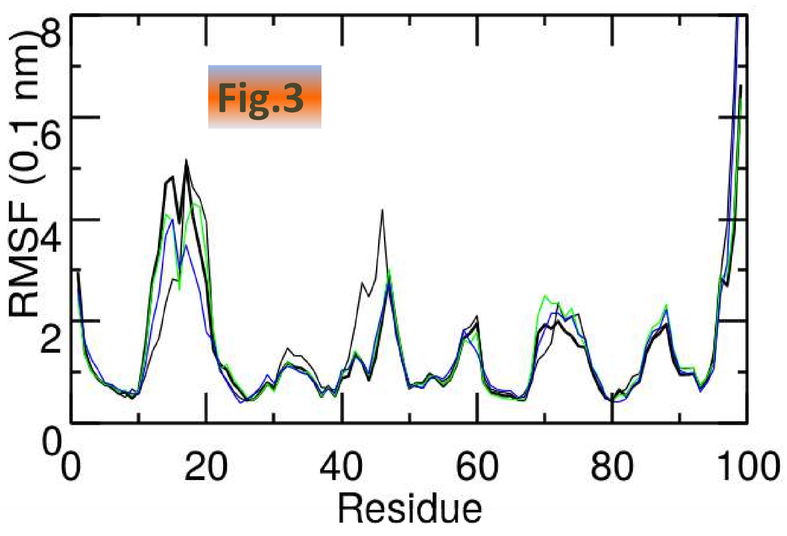

Dott. Cedrix J. Dongmo Foumthuim
Prof. Federico Fogolari

Department of Medical Area (DAME)
Tel. +39 0432 494325
Fax. +39 0432 494301
Email : dongmofoumthuim.cedrixjurgal@spes.uniud.it
Email 1 : federico.fogolari@uniud.it

SIMULATION DETAILS

The starting system with 27 copies (43848 atoms) of the protein (PDB 3hla, chain B), randomly oriented, placed at the nodes of a cubic grid (spacing 50 Å), was placed in a hydrophobic box comprising 41508 atoms. The latter was built assembling six square faces of apolar atoms which are assigned the methane united atom molecular mass 16 $gmol^{-1}$. Each square face is composed by three layers of atoms. The spacing between nearest atoms is 4.0 Å, given a length of 200 Å/side. The density is lower than that of carbon atoms in liquid alkanes by a factor 1.5 to 2.1, which implies a lower number of wall atoms in the simulation. The final system with 85356 atoms **(Fig.1)** was simulated using the Generalised Born Surface Area (GBSA) continuum solvation model of Onufriev, Bashford and Case (OBC) with amber99sb-ildn force field with gromacs-5.0.4 simulation package. Lennard Jones parameters for the apolar wall atoms have been set to σ = 0.41 nm, slightly larger than typical single aliphatic carbons and ε = 0.65 $kJmol^{-1}$, i.e. 1.4 times larger than the corresponding parameter for a methylene united atom in the force field OPLS, to partly compensate for the lower density of apolar interaction centers. The system was simulated for 62 ns and no bias was introduced.

Fig.1

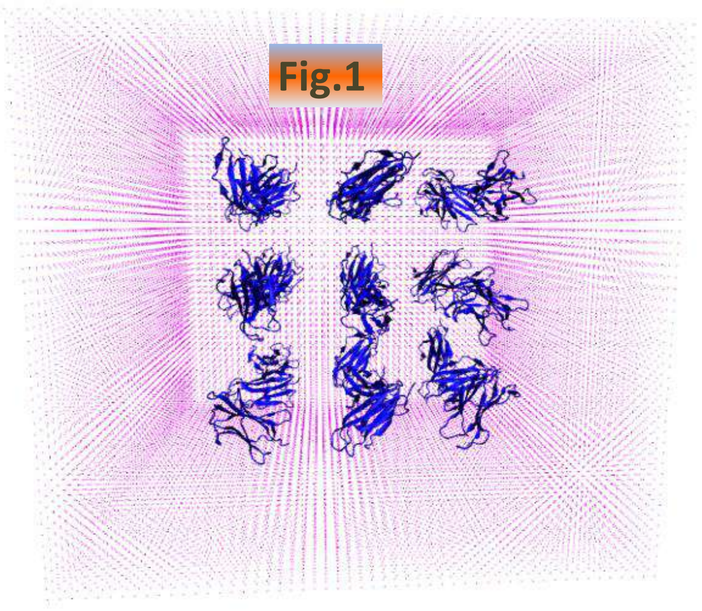

Fig.4

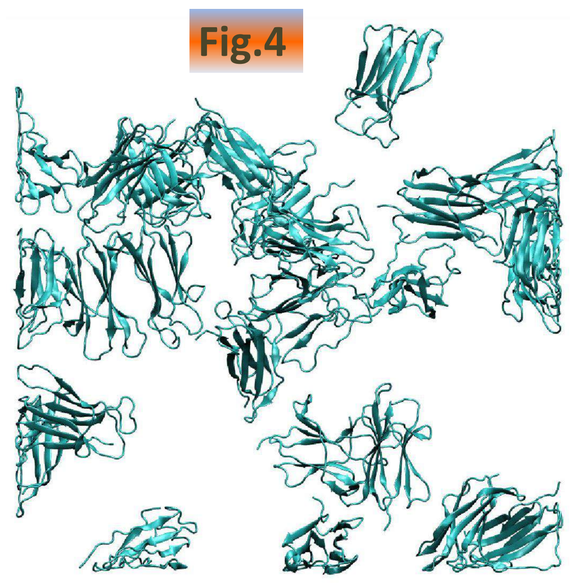

Protein adsorption and unfolding on hydrophobic walls

During the simulation 18 out of 27 molecules encounter and bind irreversibly to the walls of the bounding box, leading to large contact surface areas resulting from partial loss of secondary structure **(Fig.4)**. Strands A and G are mostly involved in partial unfolding and strand D displays conformational variability similar to that observed in NMR and crystallographic structures. It has been noted that proteins have prefered orientation upon contacting the walls. the N-terminal (Ile1, Trp60) and the C-terminal (Glu 74 , Met 99) **(Fig.5)** are the most frequent encounter sites.

Fig.5

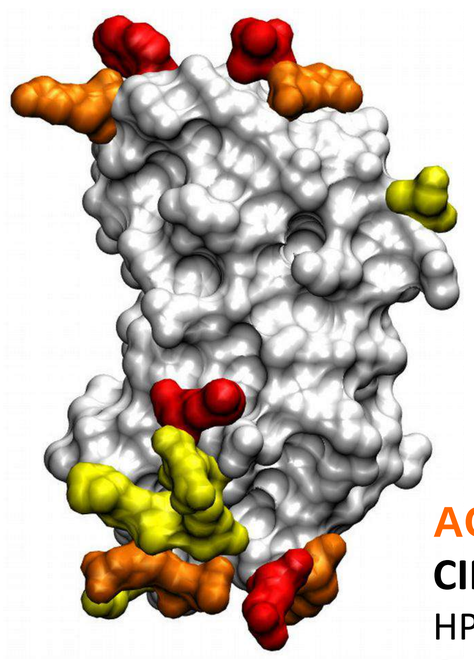

IN A NUTSHELL

Owing to the emerging role of biological interfaces occurring *in vivo* in general and in protein aggregation and fibril formation in particular, we believe our findings afford a general outlook complementary to the biochemical studies on this protein.

ACKNOWLEDGEMENTS

CINECA Projects : HP10CIWPJ4 (99,840 CPU hours) & HP10CPS5UQ (62,000 CPU hours) **PI : C. Dongmo**

BIBLIOGRAPHY

C. J. Dongmo, A. Corazza, G. Esposito, and F. Fogolari. **submitted**, 2017.

F. Fogolari, C. J. Dongmo, S. Fortuna, M. A. Soler, A. Corazza, and G. Esposito. **J. Chem. Theory Comput.**, 12:1(8), 2016.

UNIVERSITÀ DEGLI STUDI DI UDINE
hic sunt futura

LIFE SCIENCES

30° ciclo

PhD Course in Biomedical Sciences and Biotechnology

Repair of modified ribonucleotides embedded in DNA

Background

Incorporation of ribonucleotides (rNMPs) in genomic DNA is a frequent phenomenon and it could be considered the most common type of ‘DNA damage’ occurring in normal cells. This phenomenon may be due to:

- the disequilibrium in the cellular pool of rNMPs, which are much more abundant than their corresponding dNMPs counterparts;
- an incomplete elimination of RNA primers used in the generation of Okazaki fragments;
- an oxidation of the deoxyribose sugar into ribose;
- an imprecise 3’-exonucleolytic proofreading activity of replicative DNA polymerases, which do not discriminate rNMPs from dNMPs pool.

The effects of 2′-hydroxyl group of the ribose sugar of an rNMP in genomic DNA are numerous:

- it alters DNA elasticity and structure;
- it affects the activity and function of several DNA-interacting proteins;
- it increases the DNA fragility and mutability.

Applications

Considering recent works pointing to a new function of Base Excision DNA Repair (BER) in RNA surveillance, there is high likelihood that BER could be involved in the processing of rNMPs in DNA, particularly in the case of chemically modified rNMPs, such as abasic and oxidized rNMPs. Identifying whether BER may target normal and modified rNMPs in DNA is important to better understand the mechanism of genotoxicity of reactive oxygen species, the function and the impact of BER defects in human disease, cancer mechanisms and may be relevant, to an ultimate extent, for the development of new anticancer strategies.

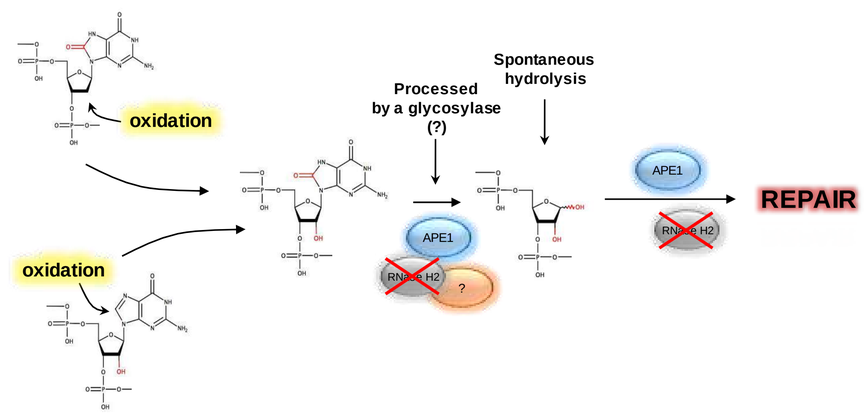

Aim of the study

Abasic rNMPs embedded in DNA may be generated by spontaneous hydrolysis or by the action of unknown glycosylases on oxidized rNMPs. Furthermore, rNMPs were shown to form during oxidative DNA damage both *in vitro* and *in vivo* or it is also possible that abasic and oxidized DNA is converted into RNA.

Our aim is finding which DNA repair pathway is deputed to repair these types of damages.

Principal Results

- Human RNase H2, belonging to Ribonucleotide Excision DNA Repair Pathway is inactive on abasic and oxidized rNMPs embedded in DNA *in vitro (1)* and *in vivo*;
- Human APE1, belonging to BER Pathway, is not able to process rNMPs embedded in DNA;
- We discovered and characterized an unknown APE1 activity on abasic and oxidized ribonucleotide embedded in DNA *in vitro (2)* and *in vivo (3)*.

(1)

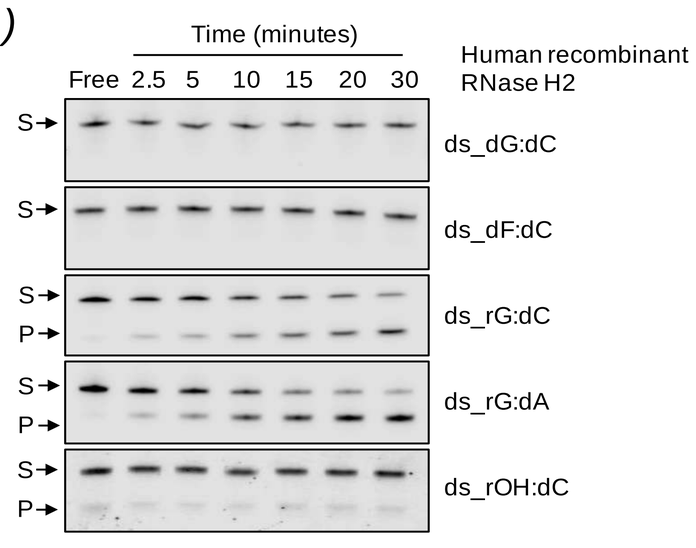

(2)

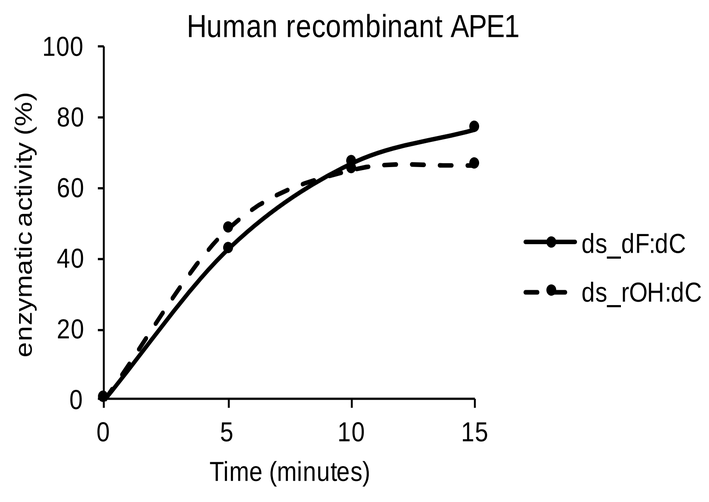

(3)

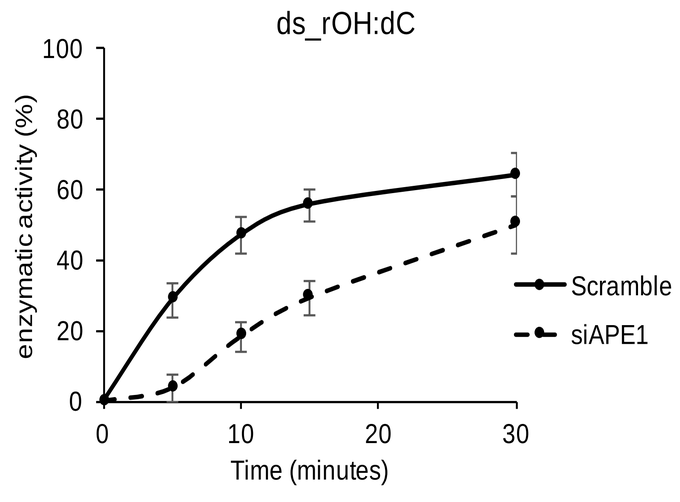

Dott. Matilde Clarissa Malfatti
Prof. Gianluca Tell

Info:
Tel. +39 0432 494313
Fax. +39 0432 494301
malfatti.matildeclarissa@spes.uniud.it

References
Malfatti *et al., under revision*
Koh *et al.,* 2015
Tell *et al.,* 2010

Acknowledgements
The authors thank the Tell and Storici laboratory for constructive feedback. They are also grateful to the funding sources by the Georgia Research Alliance, the National Institute of Health, NIH, and the Italian Association for Cancer Research, AIRC.

UNIVERSITÀ DEGLI STUDI DI UDINE
hic sunt futura

LIFE SCIENCES
30° ciclo
PhD course in Biomedical Sciences and Biotechnology

Development of anti-cancer therapies targeting RAS oncogene through non-canonical RNA structures

Introduction:

RAS ONCOGENES

Ras genes encode for a 21kDa protein involved in the regulation of many pathways controlling proliferation and cell survival. This protein function as a molecular switch between the inactive and active form. In malignant cells mutations result in a locked protein in its activated state and its constitutive activation stimulates downstream pathways responsible of many cancer hallmarks such as: enhanced proliferation, metabolic reprogramming, anti apoptotic responses, cell metastasis and migration.
RAS oncogenes are among of the most powerful cancer drivers and their mutation are present in 30% of all human cancers.

DNA/RNA G-QUADRUPLEX (G4)

G-Quadruplexes (G4) are non-canonical secondary structures that can be adopted by guanine-rich DNA and RNA molecules. They are reported to have multiple biological functions, in the genome and transcriptome of many species, including human.
The three isoforms of human Ras (HRAS, NRAS and KRAS) are similar in terms of structure and sequence: they share an high GC content and findings proved that these blocks of guanines can fold into G4 under physiological conditions. Several sudies demonstrated that the G4 in these genes/transcripts have a regulatory function suggesting the powerful role of G4 as a thepeutic target.

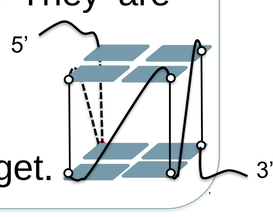

Aim of the work: DEVELOPMENT OF ANTI CANCER STRATEGIES TARGETTING RNA G4

Results:

SMALL MOLECULES

Anthrathiophenediones/ Anthrafuranediones derivatives

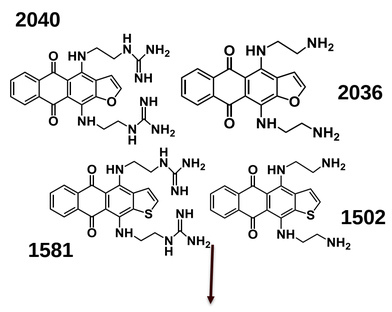

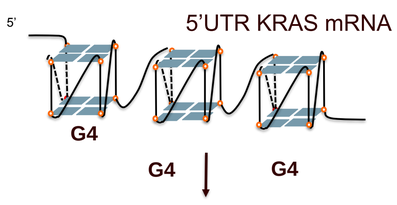

RNA G4 STABILIZATION

INHIBITION OF RAS PROTEIN TRANSLATION

PANCREATIC TUMOR CELL DEATH

Our work focus on the 5'UTR (5' untraslated region) KRAS mRNA in order to identify a target to develop an anti-cancer therapy in pancreatic cancer cells.
The 5'-UTR is very rich in guanine and by using bioinformatics tools and by experimental findings (Circular Dicroism, UV melting, EMSA and RNase footprinting) we proved that several G4 structures are formed in this tract of mRNA. We identified and characterized 3 non overlapping RNA G4s called *utr-1, utr-c* and *utr-z*.
To target the 5'-UTR G4 structures we tested a new class of small molecules: anthrathiophenediones and anthrafuranediones. By a biotin-streptavidin pull-down assay, we demonstrated that these small molecules bind to the G4s in the KRAS transcript, under its low abundance cellular conditions. Moreover Luciferase assays and western analysis showed that these small molecules repress KRAS translation.

U.V MELTING CURVES:
The melting curves analysis shows how the molecules are able to stabylize the RNA G4 conformation increasing the Tm (melting temperature) of the 3 non overlapping G4 identified in the KRAS 5'UTR. The bar chart report the ΔTm (°C) induced by increasing amounts of molecule **2036.**

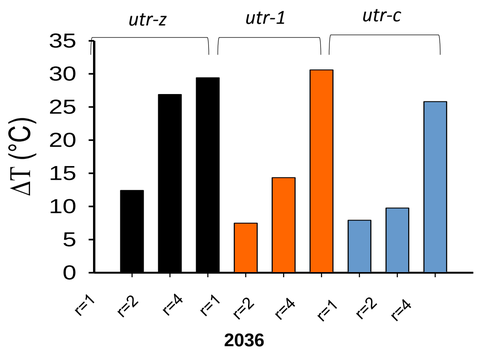

WESTERN BLOT:
The western blot performed in Panc-1 (pancreatic tumor cells) shows that the molecules (in particular **2036** and **1502**) that strongly decrease the KRAS protein if compared to not treated cells (NT).

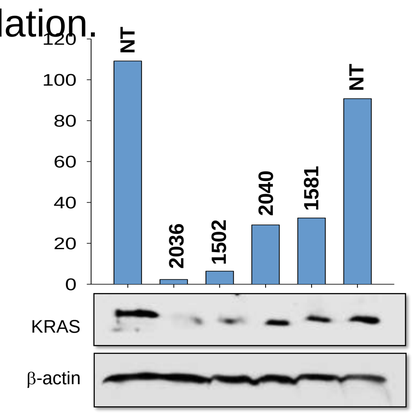

As cancer cells become addicted to the oncogene (KRAS in the pancreatic tumor) the inhibition of KRAS translation caused the activation of apoptosis and the arrest of metabolic activity.
The treatment with increasing amounts of the molecules (**2036**, **1502**, **2040** and **1581**) results in the metabolic activity arrest of Panc-1 measured by a Resazurin assay. The activation of apoptosis is confirmed by the caspase activation and the anexin-propidium assay.

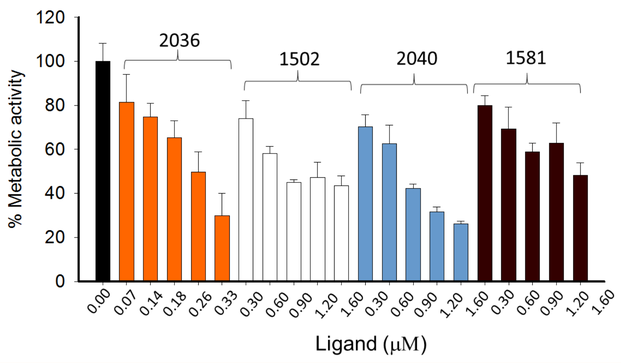

RESAZURIN ASSAY:
The bar graph sows the repression of metabolic activity in Panc-1 cells caused by the treatment with increasing concentrations of **2036**, **1502**, **2040** and **1581**. Compounds **2036** and **1502** are the most active;

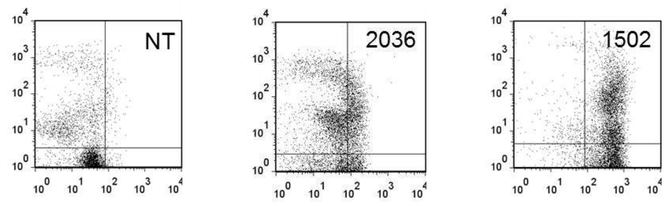

ANEXIN-PROPIDIUM ASSAY:
The anexin-propidium assay shows that in Panc-1 cells the treatment with the most active molecules **2036** and **1502** for 72h results in the increase of necrotic and apoptotic population.

Conclusions:

We showed that the human *KRAS* transcript is characterized by a GC rich 5'-UTR sequence containing 3 non-overlapping G4 structures. We have demonstrated that anthraquinones derivatives binds to G4 in the *KRAS* transcript, at its low abundance cellular level. Moreover the anthrathiophenediones and the anthrafuranediones derivatives stabylize the structure repressing KRAS translation. Ligands **2036** and **1502**, which efficiently penetrate Panc-1 cells, reduced the level of protein p21KRAS. Additionally, we found that the suppression of KRAS protein induced a strong activation of apoptosis, as determined by caspase activation and PI-annexin assays, and a dramatic reduction of cell growth.
Our work suggest a new strategy to suppress *KRAS* in pancreatic cancer cells by small molecules interacting with G4 RNA structures in 5'-UTR of KRAS transcript.

Dott. ssa Giulia Miglietta
Prof. Luigi Xodo

Info: Tel. +39 0432 494395
miglietta.giulia@spes.uniud.it
luigi.xodo@uniud.it

This work has been carried out by the financial support of AIRC:
Italian Association for Cancer Research

Bibliography:
S. Cogoi, L.E. Xodo. G4 DNA in ras genes and its potential in cancer therapy. *BiochimBiophys Acta.* 2016 Apr;1859(4):663-74

UNIVERSITÀ DEGLI STUDI DI UDINE
hic sunt futura

LIFE SCIENCES

30° ciclo
PhD course in Biomedical Sciences and Biotechnology